

Scalable and Resilient Platooning Control of Cooperative Automated Vehicles

Xiaohua Ge , Senior Member, IEEE, Qing-Long Han , Fellow, IEEE, Jun Wang , Life Fellow, IEEE, and Xian-Ming Zhang , Senior Member, IEEE

Abstract—This paper addresses the problem of distributed cooperative longitudinal control of automated vehicle platoons subject to a variety of uncertainties, including unknown engine time lags, external disturbances, measurement noises, and actuator anomaly in follower vehicles as well as unknown leader control. First, a unified framework is proposed for accomplishing resilient vehicle platooning, which empowers longitudinal vehicle state estimation, anomaly signal estimation and compensation, and adaptive platoon controller design to be addressed in a comprehensive way. Second, a novel scalable platooning control design approach is developed to guarantee desired platoon stability and resilience over generic communication topologies and various spacing policies. A salient feature of the approach is that the design procedure does not depend on any global information of the associated topology, and thus preserves essential scalability for large and/or size-varying platoons. Third, it is shown that the proposed longitudinal platooning control approach is promising for performing flexible cooperative maneuvers such as platoon splitting and merging that are beyond the capacity of most existing longitudinal platooning strategies. Finally, simulation results for different platoon maneuvers are elaborated to substantiate the efficacy of the proposed approach.

Index Terms—Autonomous vehicles, platoon maneuver, resilient control, vehicle joining, vehicle leaving, vehicle platooning.

I. INTRODUCTION

VEHICLE platooning has been regarded as a promising intelligent transportation system technology for cooperatively maneuvering an evenly spaced automated vehicle convoy on highways. Platooning offers several benefits, including improved fuel efficiency due to reduced air drag, promoted highway capacity due to small inter-vehicle distances and headways, and enhanced safety due to less drivers' distraction [1]–[3]. A primary control objective of vehicle platooning is to develop an effective distributed cooperative longitudinal control strategy such that the platoon members can establish and maintain a string formation with desired longitudinal spacing and same

Manuscript received May 26, 2021; revised November 26, 2021; accepted January 24, 2022. Date of publication February 1, 2022; date of current version May 2, 2022. This work was supported by the Research Grants Council of the Hong Kong Special Administrative Region of China through General Research Fund under Grants 11202318 and 11203721. The review of this article was coordinated by Dr. Theo Hofman. (*Corresponding author: Qing-Long Han.*)

Xiaohua Ge, Qing-Long Han, and Xian-Ming Zhang are with the School of Science, Computing and Engineering Technologies, Swinburne University of Technology, Melbourne, VIC 3122, Australia (e-mail: xge@swin.edu.au; qhan@swin.edu.au; xiammingzhang@swin.edu.au).

Jun Wang is with the Department of Computer Science, School of Data Science, City University of Hong Kong, Hong Kong (e-mail: jwang.cs@cityu.edu.hk).

Digital Object Identifier 10.1109/TVT.2022.3147371

velocity (and acceleration) with the platoon leader. Adaptive cruise control (ACC) represents a typical platooning technology for achieving such a longitudinal platoon tracking control objective and is extensively applied to modern commercial vehicles. However, ACC-enabled vehicles use solely onboard sensing devices, such as radar and scanning lidar, to realize a desired inter-vehicle distance. As a result, an ACC-based vehicular platoon usually keeps a relatively large spacing between adjacent vehicles, thereby resulting in degraded highway capacity utilization.

With the rapid development of wireless communication technology, the standard ACC has been upgraded to cooperative adaptive cruise control (CACC). What distinguishes CACC from ACC is the introduction of wireless communication such that the CACC-equipped vehicles can communicate with their ‘neighbors’ by exchanging their useful data (e.g., position, velocity, acceleration) via wireless vehicle-to-everything (V2X) communication. Depending on platoon scenarios, the ‘neighbors’ can be characterized by adjacent vehicles via vehicle-to-vehicle (V2V) communication or roadside infrastructure (e.g., roadside units) via vehicle-to-infrastructure (V2I) communication or pedestrians via vehicle-to-pedestrian (V2P) communication. Owe to the additional wireless V2V information exchanges beyond line-of-sight of onboard sensors, CACC-based longitudinal control strategies can ensure satisfactory platooning performance under smaller inter-vehicle distances, without compromising safety, in comparison to ACC counterparts. Up until now, a variety of V2V communication topologies, as shown in Fig. 1, have been studied for cooperative longitudinal control of automated vehicle platoons with the aid of the mature IEEE 802.11p-based dedicated short range communication technology and the emerging 5G cellular communication technology.

The platoon performance of CACC-equipped vehicles is closely related to the adopted V2V communication topology, because the wireless V2V communication enables the intelligent vehicles to learn about the dynamics and behaviors of their surrounding vehicles. Besides, platoon vehicles rely on the exchanged information between neighboring vehicles to achieve and maintain the desired collective platoon behavior. For example, the well-known California Partners for Advanced Transit and Highways (PATH) program demonstrates that under a leader-predecessor-following (LPF) topology (i.e., each vehicle receives information from both the leading vehicle and its preceding vehicle), the platoon is capable of successfully maintaining string stability and constant spacing [4]. A platoon controller synthesis method is presented in [5] for evaluating the string stability requirement under a predecessor-following (PF) topology (or one-vehicle look-ahead topology) and a two

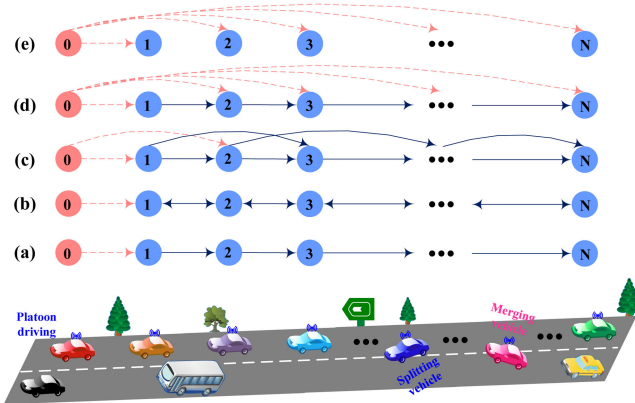


Fig. 1. Five typical V2V communication topologies of automated platoon maneuvering on a stretch of highway: (a) a predecessor-following (PF) topology; (b) a bidirectional (BD) topology; (c) a two predecessor-following (TPF) topology; (d) A leader-predecessor-following (LPF) topology; and (e) a leader-following (LF) topology.

predecessor-following (TPF) topology (or two-vehicle look-ahead topology). It is shown that a multiple-vehicle look-ahead topology is beneficial for the platoon to preserve the minimum string-stable time headway under a large communication delay. In [6], a fault-tolerant platooning control scheme is devised for a vehicular platoon connected over a PF communication topology to deal with actuator faults. In [7], an optimal platooning control approach is proposed for CACC-enabled vehicles under a PF topology in the presence of actuator delays, communication delays, and data packet dropouts. The disturbance scaling of vehicle platoons over a bidirectional (BD) topology is studied in [8], where each platoon vehicle can gather information of its direct preceding and following vehicles. It reveals that the platoon performance can be improved by allowing symmetric position coupling and asymmetric velocity coupling in local control law. A switching control method is put forward in [9] for vehicle platoons over a leader-following (LF) topology, where the connectivity status between the leader and each follower varies over time. It is worth noting that the aforementioned platooning control strategies are designed on the basis of specific topologies, which might limit their application scopes for platooning requirements over various topologies.

By virtue of algebraic graph theory, a consensus strategy is intensively studied for vehicle platooning control, aiming to cover general topologies; see, e.g., [10]–[19] and the references therein. From a graph-theoretic perspective, it is well acknowledged that the eigenvalues of either the adjacency matrix \mathcal{A} , the Laplacian \mathcal{L} , and the \mathcal{H} matrix (consisting of the Laplacian \mathcal{L} and the leader pinning matrix \mathcal{A}_0) essentially represent some global knowledge of the graph (and thus the V2V communication topology). However, the vast majority of the existing platooning controller design approaches necessitate such global information of the associated communication topologies (either undirected or directed) during platoon controller design, such as all eigenvalues of \mathcal{L} [10], the nonzero minimal eigenvalue of \mathcal{H} [11]–[13], all eigenvalues of \mathcal{H} [14]–[17], the maximal and minimal eigenvalues of \mathcal{H} [18], the maximal and minimal eigenvalues of the \mathcal{A} -related matrix [19]. Such requirements intrinsically make them not practically preferable during flexible platoon maneuvers or not implementable in every follower vehicle in a fully

distributed fashion. For example, during platoon maneuvers with dynamic joining and leaving vehicles, the size of the platoon and the V2V communication topology structure inevitably vary from time to time. In this case, those platoon controllers might be no longer capable to guarantee the desired platoon stability and performance in the event of changing platoon configurations and communication topologies. Hitherto it remains challenging to develop an inherently scalable platooning control approach for each platoon vehicle to regulate its motion during platoon maneuvers without any global knowledge of the underlying communication topology.

In this paper, we address the scalable and resilient platooning control of an CACC-equipped automated vehicle convoy subject to various uncertainties. The novelty of the work lies in the development of an essentially scalable and resilient platooning control approach over a communication network of a generic V2V topological structure such that the platoon can be controlled in a truly distributed manner, in the presence of different types of uncertainties. The main contributions are summarized as follows.

1) *A unified framework for resilient platooning control* is established, which enables vehicle state estimation, anomaly signal estimation and compensation, and adaptive controller design for the platoon to be investigated comprehensively. Specifically, a general longitudinal vehicle dynamical model is considered, in the simultaneous presence of unknown engine time lags, external disturbances, measurement noise, and actuator anomaly on every follower vehicle as well as an unknown leader control input. Then, local state observers are developed for each follower vehicle based on only noisy sensor position measurements to estimate unavailable full vehicular states and anomaly signals.

2) *A novel scalable adaptive platooning control approach* is developed for the platoon operated over generic V2V communication topologies. The proposed control approach exhibits two main features: i) the design procedure is offline, decoupled from the topology, independent of any global information of the topology, and thus essentially scalable for size-variant platoons. This marks a distinction between this paper and most of the existing platooning control approaches that depend on the eigenvalues of the relevant graph matrices. Furthermore, owing to the salient scalability feature, the designed platoon controllers do not need to be redesigned or reconfigured when the platoon size and topology structure vary, which represents a promising strategy for cooperative maneuvering; and ii) the local control law for each follower vehicle can adaptively adjust its gains such that the large platoon tracking error, caused by uncertainties, can be accommodatively restrained.

3) *Rigorous stability analysis of the resulting estimation error system and platoon tracking error system* is provided. Note that the co-existence of various types of uncertainties poses a significant challenge for the platoon to exhibit desired accurate platoon stability. It is analytically proved that the tracking and spacing errors of the platoon are guaranteed to be convergent to some small neighborhoods around zero.

4) *Efficient platoon maneuver algorithms* are proposed to enable flexible platoon maneuvers, including vehicle driving, joining, and leaving. Albeit platoon stability and resilience are important aspects that one should account for during the cooperative longitudinal motion control, it is noted that vehicle platoons, in most situations, travel on highways in the presence of other non-platooned vehicles. It means that practical platoon maneuvers should enjoy flexible ‘cut-in’ and ‘cut-through’

operations such as vehicle joining and leaving to meet the mobility needs. However, it is stressed that the flexible platoon maneuvers are inherently challenging for at least two main reasons: 1) a platoon is required to change its formation (or spacing), which implies that a feasible platoon control law needs to guarantee a smooth transition between two formations, and also to efficiently open/close the inter-vehicle gaps due to the joining/leaving vehicles; and 2) the platoon stability and resilience, as pursued in this paper, still demand to be well maintained for the newly expanded/reduced platoon. Besides, platoon maneuvering generally requires dedicated lateral control efforts and also suitable management protocols for warranting transient phases; see, e.g., the survey [20] on the topics of lane change and merging. Although lateral control is not a focus of this paper, it is shown that the proposed longitudinal platooning control approach incorporates some built-in properties for flexible leaving and joining maneuvers, and thus provides a certain level of cooperative automated maneuvering.

The remainder of this paper is organized as follows. The preliminaries and the problem of interest are introduced in Section II. The main results in terms of platoon controller design, stability analysis and platoon maneuvering algorithms are provided in Section III. The effectiveness of the proposed platooning control method is demonstrated through several numerical experiments in Section IV. Section V presents some concluding remarks.

II. PRELIMINARIES AND PROBLEM FORMULATION

A. Notations

For a symmetric matrix Φ , $\Phi > 0$ means that it is positive definite. The transpose of a matrix (vector) Φ is denoted by Φ^T . If a matrix is invertible, the superscript “ -1 ” represents the matrix inverse. For a matrix Φ , denote $\underline{\sigma}(\Phi)$ and $\overline{\sigma}(\Phi)$, respectively, as its minimum and maximum singular values. For a real, positive definite, and symmetric matrix Φ , denote $\underline{\lambda}(\Phi)$ and $\overline{\lambda}(\Phi)$, respectively, as its minimum and maximum eigenvalues. $\mathbf{1} = [1, 1, \dots, 1]^T$ stands for the column vector of an appropriate dimension. \mathbf{I} represents the identity matrix of an appropriate size. $\mathbf{0}$ represents the zero vector or matrix of an appropriate size. $\text{diag}\{\Phi_1, \Phi_2, \dots, \Phi_m\}$ is used to denote an m -block diagonal matrix with Φ_i , $\forall i = 1, 2, \dots, m$, being the i -th diagonal element. $\|\cdot\|$ denotes the Euclidean norm of a vector. \otimes denotes the Kronecker product. Matrices, if not explicitly stated, are assumed to have compatible dimensions.

B. Uncertain Vehicle Longitudinal Dynamics

Consider a platoon consisting of $N + 1$ automated vehicles, where the leader vehicle is labeled as $i = 0$ and the follower vehicles are indexed by $i = 1, 2, \dots, N$. For any $i \in \tilde{\mathcal{V}} = \{0, 1, 2, \dots, N\}$, let $p_i(t)$, $\dot{p}_i(t)$, $\ddot{p}_i(t)$, $\dddot{p}_i(t)$ denote the longitudinal position, velocity, acceleration and jerk of the i -th vehicle, respectively. Then, the longitudinal dynamics can be described by the following state-space equation:

$$\tau_i \ddot{p}_i(t) + \ddot{p}_i(t) = u_i(t) + \tilde{w}_i(t), i \in \tilde{\mathcal{V}}, \quad (1)$$

where τ_i represents the unknown engine inertial delay, $u_i(t)$ stands for the desired control input, and $\tilde{w}_i(t)$ denotes the unknown external disturbance input. To cope with the unknown heterogeneous delay τ_i , one may rewrite it as $\tau_i = \tau_e + \tilde{\tau}_i$,

where τ_e denotes the nominal part and $\tilde{\tau}_i$ represents the uncertain part. Then, by introducing the augmented state vector $x_i(t) = [p_i(t), \dot{p}_i(t), \ddot{p}_i(t)]^T$ and defining $w_i(t) = \tilde{w}_i(t) - \tilde{\tau}_i \ddot{p}_i(t)$, $i \in \tilde{\mathcal{V}}$, the longitudinal dynamics in (1) can be rewritten as

$$\dot{x}_i(t) = Ax_i(t) + B(u_i(t) + w_i(t)), i \in \tilde{\mathcal{V}}, \quad (2)$$

where

$$A = \begin{bmatrix} 0 & 1 & 0 \\ 0 & 0 & 1 \\ 0 & 0 & -\frac{1}{\tau_e} \end{bmatrix}, B = \begin{bmatrix} 0 \\ 0 \\ \frac{1}{\tau_e} \end{bmatrix}.$$

Note that the longitudinal model (2) offers a general description of vehicle longitudinal dynamics than the existing deterministic and homogeneous longitudinal vehicle models in terms of $\tilde{w}_i(t) \equiv 0$ and $\tau_i \equiv \tau_e$ in (1) (see, e.g., [5], [9], [10], [12], [14], [15], [19], [21]). For the leader vehicle, it is assumed that $w_0(t) = 0$, however, its control input $u_0(t)$ allows to be nonzero and time-varying, which makes the platooning control problem more involved than the case of $u_0(t) \equiv 0$ [8]–[12], [19], [21].

C. Actuator Anomaly

During practical platoon maneuvering, the actuator (throttle/brake) of a vehicle may operate unreliably due to some unpredictable mechanical and electronic faults. On the other hand, automated vehicles adopt a number of essential engine control units (ECUs), such as engine control module, electronic brake control module, transmission control module, to maintain autonomous control functionality [22]. These ECUs, however, face constant security threats from external adversaries. This is because the reliable and safe operations of the ECUs, which play a crucial role in vehicle dynamics control systems, are common targets of attackers to disrupt the functionality of a vehicle. For example, the ECU responsible for acquiring and processing wheel speed can be compromised by a remote hacker to cause incorrect braking [23]. Based on the observations above, for any $i \in \mathcal{V}$, we consider the following realistic actuator model

$$u_i(t) = \tilde{u}_i(t) + m_i(t), \quad (3)$$

where $\tilde{u}_i(t)$ is the desired adaptive control input to be designed and $m_i(t)$ represents the unknown actuator anomaly signal corrupting the desired control commands, which could be caused by benign faults or malicious attacks.

D. Time-Varying Spacing Policies

The main issue in a longitudinal platooning controller design is to determine a desired distributed coordination control law $u_i(t)$, $i \in \mathcal{V}$, such that the N follower vehicles gradually reach the same speed and acceleration as the leader 0, i.e.,

$$\dot{p}_i(t) - \dot{p}_0(t) \rightarrow 0, \ddot{p}_i(t) - \ddot{p}_0(t) \rightarrow 0, \text{ as } t \rightarrow \infty, \quad (4)$$

while simultaneously maintaining a desired longitudinal spacing between any two adjacent vehicles; viz., the spacing error $\psi_i(t)$ satisfies

$$\psi_i(t) = p_{i-1}(t) - p_i(t) - d_{i-1,i}(t) \rightarrow 0, \text{ as } t \rightarrow \infty, \quad (5)$$

where $d_{i-1,i}(t) = d_{i-1}^0(t) - d_i^0(t)$ denotes the anticipated spacing between follower i and its predecessor $i - 1$ at time t . Given the various uncertainties in the vehicular longitudinal dynamics (2), however, it is difficult to accomplish accurate

platoon stability in an asymptotic way. To make the proposed platooning control problem clear, we define the platoon tracking error for follower vehicle i as

$$e_i(t) = x_i(t) - d_i(t) - x_0(t), \forall i \in \mathcal{V}, \quad (6)$$

where $d_i(t) = [d_i^0(t), 0, 0]^T$ is the designated spacing vector associated with follower vehicle i with $d_i^0(t)$ being a piecewise continuously differentiable function that specifies the anticipated distance between the follower vehicle i and the leader vehicle 0. Then, the following definition describes the expected platoon tracking control objective.

Definition 1: For the vehicular platoon with uncertain longitudinal dynamics (2), the N follower vehicles with the desired control law $u_i(t)$ achieve the *resilient platoon tracking* of the leader 0 if $\lim_{t \rightarrow \infty} \|e_i(t)\| \leq \delta_i, \forall i \in \mathcal{V}$, where δ_i denotes a small positive scalar.

Remark 1: The time-varying vector $d_i(t)$ in Definition 1 can be customized to suit different spacing requirements for the platoon vehicles. For example, by setting $d_i^0(t) = i \cdot d_0$ for any $i \in \mathcal{V}$, it leads to a constant spacing policy [8]–[15], [24], [25], where d_0 is the prescribed inter-vehicle distance; by letting $d_i^0(t) = h_i v_i(t) + s_i$, a constant time headway spacing policy [5], [19], [21], [26]–[29] is captured by $d_i(t)$ as a special case, where h_i denotes the time headway constant and s_i denotes the desired distance between vehicle i and vehicle 0 at standstill. The subsequent analysis and design herein are not confined to some specific spacing policy. Instead, we focus on the general piecewise or continuously differentiable function $d_i^0(t)$, because various formations and thus variable spacing requirements are demanded for flexible platoon maneuvers such as vehicle leaving and joining.

E. Local Vehicular State Observers

Instead of requiring the full state $x_i(t)$ of each vehicle to accomplish the platoon control design, we aim at constructing and designing some local observers for the follower vehicles based on only position measurements. More specifically, for each vehicle i , the sensor measurement model is given as

$$y_i(t) = Cx_i(t) + Dv_i(t), \forall i \in \mathcal{V}, \quad (7)$$

where $y_i(t)$ denotes the sensor measurement recorded by the on-board sensing module of each platoon vehicle; $v_i(t)$ denotes the unknown measurement noise; $C = [1, 0, 0]$; and D is a prescribed scalar. Clearly, only the position measurement of each follower vehicle is required in the subsequent analysis and design. In practice, the vehicular position measurement can be readily obtained via a global navigation satellite system and inertial navigation system (GNSS/INS) component of the automated vehicle.

The local state observer deployed on each follower vehicle i in the platoon takes the following form

$$\begin{cases} \dot{\hat{x}}_i(t) = (A + LC)\hat{x}_i(t) + B(\tilde{u}_i(t) + \hat{m}_i(t)) - Ly_i(t), \\ \dot{\hat{m}}_i(t) = FC\hat{x}_i(t) - Fy_i(t), \end{cases} \quad (8)$$

where $\hat{x}_i(t) = [\hat{p}_i(t), \dot{\hat{p}}_i(t), \ddot{\hat{p}}_i(t)]^T$ denotes the state estimate of the full vehicular state $x_i(t)$; $\hat{m}_i(t)$ is an estimate of the unknown anomaly signal $m_i(t)$; $\tilde{u}_i(t)$ denotes an adaptive control input signal to be specified later; L and F are the observer gain matrices to be designed.

F. V2V Communication

For a CACC-enabled vehicular platoon, each vehicle equips an on-board wireless transceiver, permitting its local vehicle information to be shared with its underlying neighbors in accordance with a suitable V2V communication topology. Specifically, we consider that the local state estimate $\hat{x}_i(t)$ on each vehicle $i, i \in \mathcal{V}$, is shared with its neighbors over the V2V communication topology, which is much less demanding than exchanging the full vehicular state $x_i(t)$ of each follower vehicle. This is because the complete information of $x_i(t)$ is not precisely accessible for each platoon vehicle at time t . For example, it is costly to obtain the accurate acceleration information $\ddot{p}_i(t)$ of a high-speed moving vehicle in practical situations.

Considering each follower vehicle as a node in a graph \mathcal{G} , we model the V2V communication network of N follower vehicles by using a weighted digraph $\mathcal{G} = (\mathcal{V}, \mathcal{E}, \mathcal{A})$, where $\mathcal{V} = \{1, 2, \dots, N\}$ denotes an index set of N nodes (vehicles), $\mathcal{E} \subseteq \mathcal{V} \times \mathcal{V}$ denotes an edge set of paired nodes with (j, i) representing a directional edge (information link) from node j to node i , and $\mathcal{A} = [a_{ij}] \in \mathbb{R}^{N \times N}$ denotes a weighted adjacency matrix with $a_{ij} \geq 0$ being the adjacency element (weight) of the edge (j, i) . It is assumed that self-loops are excluded in the graph; i.e., $a_{ii} = 0$ for any $i \in \mathcal{V}$. A path of \mathcal{G} is a concatenation of directed edges $\{(i_1, i_2), (i_2, i_3), \dots, (i_{p-1}, i_p)\} \in \mathcal{E}$, in which all nodes i_1, i_2, \dots, i_p are distinct. The digraph \mathcal{G} has a spanning tree if there exists at least one node, called the root, such that there is a path from this node to any other node in the graph. The Laplacian matrix associated with the digraph \mathcal{G} is defined as $\mathcal{L} = \mathcal{D} - \mathcal{A}$, where $\mathcal{D} = \text{diag}\{d_1, d_2, \dots, d_N\}$ with $d_i = \sum_{j=1}^N a_{ij}$.

Let $\tilde{\mathcal{G}} = (\tilde{\mathcal{V}}, \tilde{\mathcal{E}}, \tilde{\mathcal{A}})$ denote an augmented digraph consisting of the digraph \mathcal{G} and an extra node 0 acting as the leader node, where $\tilde{\mathcal{V}} = \mathcal{V} \cup \{0\}$, $\tilde{\mathcal{E}} \subseteq \tilde{\mathcal{V}} \times \tilde{\mathcal{V}}$, and $\tilde{\mathcal{A}} = [a_{ij}] \in \mathbb{R}^{(N+1) \times (N+1)}$. It is assumed that only a subset of nodes in $\tilde{\mathcal{G}}$ can receive information from node 0 while node 0 does not receive information from any node in \mathcal{G} , meaning that $a_{0j} \equiv 0$ for any $j \in \tilde{\mathcal{V}}$. Moreover, $a_{i0} > 0, \forall i \in \mathcal{V}$, if and only if the i -th node in \mathcal{G} has a directional edge to the leader node 0; namely, node i is pinned by the leader node; otherwise $a_{i0} = 0$. Let $\mathcal{A}_0 = \text{diag}\{a_{10}, a_{20}, \dots, a_{N0}\}$ denote the pinning matrix of the leader node and $\mathcal{H} = \mathcal{L} + \mathcal{A}_0$.

Assumption 1: There is a spanning tree rooted at the leader node 0 in the augmented digraph $\tilde{\mathcal{G}}$.

Lemma 1: [30] Under Assumption 1, the matrix \mathcal{H} is non-singular and there exists a diagonal matrix $\mathcal{T} = \text{diag}\{\tau_1, \tau_2, \dots, \tau_N\} = \text{diag}\{q_1^{-1}, q_2^{-1}, \dots, q_N^{-1}\} > 0$ such that $G = \mathcal{T}\mathcal{H} + \mathcal{H}^T\mathcal{T} > 0$, where the positive scalars q_i can be determined from $\bar{q} = [q_1, q_2, \dots, q_N]^T = \mathcal{H}^{-1}\mathbf{1}$.

Remark 2: The V2V communication network, characterizing how information sharing is performed among the connected vehicles, plays a vital role in the successful achievement of the desired cooperative platooning control objective. The choice of a suitable V2V communication topology has a significant impact on the platoon behaviors. In this study, however, we do not confine our attention to any specific communication network topology, but instead place an emphasis on a generic topological structure under Assumption 1. As a matter of fact, Assumption 1 accommodates a variety of V2V topologies used in the existing platooning control literature. For example, all typical V2V communication topologies shown in Fig. 1 satisfy Assumption 1. We herein devote ourselves to developing a novel scalable

and resilient platooning control approach that accommodates various V2V communication topologies.

G. The Problem to Be Addressed

The *scalable and resilient vehicle platooning control problem* to be addressed is stated as follows: For the uncertain vehicular platoon described in (2) over a generic communication topology $\tilde{\mathcal{G}}$ satisfying Assumption 1, under a desired spacing policy specified by $d_i(t)$, the objective is to design scalable and resilient platooning control laws $\tilde{u}_i(t)$ based on the local state observers in (8) such that the platoon tracking errors $e_i(t)$ and the spacing errors $\psi_i(t)$ converge to some small neighborhoods around zero for all $i \in \mathcal{V}$.

III. MAIN RESULTS

In this section, we first elaborate on the desired scalable and resilient platooning control laws. Next we present the detailed design procedure for determining the observer and controller gain parameters. Then we derive the resulting estimation error and tracking error systems, and perform formal stability analysis by proving that all variables in the error systems are uniformly ultimately bounded. Finally, we demonstrate flexible platoon maneuvers under the proposed platooning approach.

A. Scalable and Resilient Platoon Tracking Control Laws

We aim to design the following scalable and resilient distributed control law for each follower vehicle without any global information about the V2V network topology $\tilde{\mathcal{G}}$:

$$\tilde{u}_i(t) = \alpha_i(t)\rho_i(\eta_i^T(t)Q\eta_i(t))K\eta_i(t) - \hat{m}_i(t), \quad (9)$$

where $\alpha_i(t)$ is a time-varying coupling gain to be determined and satisfies $\alpha_i(0) \geq 1$, $\rho_i(\cdot)$ is a smooth and monotonically increasing function to be specified later and satisfies $\rho_i(s) \geq 1$ for $s > 0$, K denotes a feedback control gain matrix to be designed, and $\eta_i(t)$ represents the local neighborhood tracking error defined as

$$\eta_i(t) = \sum_{j \in \tilde{\mathcal{V}}} a_{ij} (\hat{x}_i(t) - d_i(t) - (\hat{x}_j(t) - d_j(t))). \quad (10)$$

In (9), the fault estimate $\hat{m}_i(t)$ is employed to compensate the effect of the unknown actuator anomaly in follower vehicle i .

B. Estimation Error and Tracking Error Dynamics

For each follower vehicle i , $i \in \mathcal{V}$, we define the state and anomaly estimation errors as

$$\tilde{x}_i(t) = \hat{x}_i(t) - x_i(t), \tilde{m}_i(t) = \hat{m}_i(t) - m_i(t), \quad (11)$$

and the estimate tracking error as

$$\delta_i(t) = \hat{x}_i(t) - d_i(t) - x_0(t). \quad (12)$$

For brevity, we may sometimes drop the time argument (t) hereinafter, with the understanding that all the variables in the error dynamics are time-dependent, whenever without causing any confusion.

Substituting (9) into (2) and (8), and in view of (3), (11) and (12), we obtain the following estimation error dynamic equation:

$$\dot{\xi}_i = \tilde{A}\xi_i + \tilde{E}\tilde{w}_i, i \in \mathcal{V}, \quad (13)$$

where $\xi_i = [\tilde{x}_i^T, \tilde{m}_i^T]^T$, $\tilde{w}_i = [w_i^T, v_i^T, \dot{m}_i^T]^T$, and

$$\tilde{A} = \begin{bmatrix} A + LC & B \\ FC & 0 \end{bmatrix}, \tilde{E} = \begin{bmatrix} -B & -LD & \mathbf{0} \\ 0 & -FD & -1 \end{bmatrix}.$$

On the other hand, in view of the local tracking error in (12), the neighborhood tracking error η_i in (10) can be rewritten as

$$\eta_i = \sum_{j \in \tilde{\mathcal{V}}} a_{ij}(\delta_i - \delta_j). \quad (14)$$

To obtain a compact form of the desired tracking error dynamics, we denote by $\tilde{x} = [\tilde{x}_1^T, \tilde{x}_2^T, \dots, \tilde{x}_N^T]^T$, $\delta = [\delta_1^T, \delta_2^T, \dots, \delta_N^T]^T$, $\eta = [\eta_1^T, \eta_2^T, \dots, \eta_N^T]^T$, $\tilde{u}_0 = \mathbf{1} \otimes u_0$, $\dot{d} = [d_1^T, d_2^T, \dots, d_N^T]^T$, $v = [v_1^T, v_2^T, \dots, v_N^T]^T$, $\alpha = \text{diag}\{\alpha_1, \alpha_2, \dots, \alpha_N\}$, and $\rho = \text{diag}\{\rho_1, \rho_2, \dots, \rho_N\}$. Substituting (9) into (8) and in view of (2) and (14), we obtain the following platoon tracking error dynamic equation:

$$\dot{\delta} = (\mathbf{I} \otimes A + \alpha \rho \mathcal{H} \otimes BK) \delta + (\mathbf{I} \otimes LC) \tilde{x} + \bar{\varpi}, \quad (15)$$

where $\bar{\varpi} = -(\mathbf{I} \otimes B) \tilde{u}_0 - \dot{d} - (\mathbf{I} \otimes (LD))v$. From (14), it can be derived that $\eta = (\mathcal{H} \otimes \mathbf{I})\delta$. Then we obtain the following neighborhood tracking error dynamic equation:

$$\dot{\eta} = (\mathbf{I} \otimes A + \mathcal{H} \alpha \rho \otimes BK) \eta + (\mathcal{H} \otimes LC) \tilde{x} + \varpi, \quad (16)$$

where $\varpi = -(\mathcal{H} \otimes B) \tilde{u}_0 - (\mathcal{H} \otimes \mathbf{I})\dot{d} - (\mathcal{H} \otimes (LD))v$.

C. A Three-Step Design Procedure

The following procedure outlines the design of the observer-based distributed platoon tracking control laws (8) and (9) for the vehicular platoon (2).

Step 1: Determine the local observer gain matrices L and F in (8), and derive the estimates $\hat{x}_i(t)$ and $\hat{m}_i(t)$. Consider the following Riccati matrix equation:

$$\tilde{P}\tilde{A} + \tilde{A}^T\tilde{P} + \frac{1}{\beta_0}\tilde{P}\tilde{E}\tilde{E}^T\tilde{P} = -U, \quad (17)$$

where $\tilde{P} = \begin{bmatrix} P_{11} & P_{12} \\ * & P_{22} \end{bmatrix} > 0$ and $U > 0$ are real matrices, $\beta_0 > 0$ is a scalar. Applying Schur complement [31], we have

$$\begin{bmatrix} \Xi_1 + \Xi_1^T & \Xi_2 \\ * & -\beta_0 \mathbf{I} \end{bmatrix} < 0,$$

where

$$\Xi_1 = \begin{bmatrix} P_{11}(A + LC) + P_{12}FC & P_{11}B \\ P_{12}^T(A + LC) + P_{22}FC & P_{12}^TB \end{bmatrix},$$

$$\Xi_2 = \begin{bmatrix} -P_{11}B - P_{11}LD - P_{12}FD - P_{12} \\ -P_{12}^TB - P_{12}^TLD - P_{22}FD - P_{22} \end{bmatrix}.$$

Note that the observer gain matrices L , F and the Lyapunov matrices P_{11} , P_{12} , P_{22} are coupled in the above matrix inequality. To address this, we subtly choose $P_{11} = \check{P} + \kappa_1 P_{12}P_{12}^T$, $P_{12} = -\kappa_2 B$, $P_{22} = \kappa_1^{-1}$, $F = -\kappa_1 P_{12}^T L$, $\check{P} = \check{P}L$. Then, for given scalars $\kappa_1 > 0$ and κ_2 , if there exist matrices $\check{P} > 0$, \hat{P} , and a scalar $\beta_0 > 0$ such that

$$\begin{bmatrix} \tilde{\Xi}_1 & \tilde{\Xi}_2 \\ * & -\beta_0 \mathbf{I} \end{bmatrix} < 0, \quad (18)$$

where

$$\begin{aligned}\tilde{\Xi}_1 &= \begin{bmatrix} \check{P}A + A^T\check{P} + \hat{P}C + C^T\hat{P}^T & \tilde{\Xi}_3 - \kappa_2 A^T B \\ +\kappa_1\kappa_2^2(BB^TA + A^TBB^T) & * \\ * & -2\kappa_2 B^T B \end{bmatrix}, \\ \tilde{\Xi}_2 &= \begin{bmatrix} -\tilde{\Xi}_3 & -\hat{P}D & \kappa_2 B \\ \kappa_2 B^T B & 0 & -\kappa_1^{-1} \end{bmatrix}, \\ \tilde{\Xi}_3 &= \check{P}B + \kappa_1\kappa_2^2 BB^T B,\end{aligned}$$

then we obtain that $L = \check{P}^{-1}\hat{P}$ and $F = \kappa_1\kappa_2 B^T \check{P}^{-1}\hat{P}$.

Based on the local observer (8), the vehicle state estimate $\hat{x}_i(t)$ and the actuator anomaly estimate $\hat{m}_i(t)$ for each follower vehicle i , $i \in \mathcal{V}$, can be derived.

Step 2: Determine the feedback control gain matrix K and the adaptive weighting matrix S . Solve the following Riccati matrix equation:

$$QA + A^TQ - 2QBB^TQ = -V, \quad (19)$$

to determine the positive definite matrix Q , where $V > 0$ is a real matrix. Compute the matrices $K = -B^TQ$ and $S = QBB^TQ$.

Step 3: Determine the scalable and resilient control laws $\tilde{u}_i(t)$. The desired adaptive control input $\tilde{u}_i(t)$ on vehicle i is defined by the following equations:

$$\begin{cases} \tilde{u}_i(t) = \alpha_i(t)\rho_i(\eta_i^T(t)Q\eta_i(t))K\eta_i(t) - \hat{m}_i(t), \\ \dot{\alpha}_i(t) = \eta_i^T(t)S\eta_i(t) - \gamma_i(\alpha_i(t) - 1), \\ \rho_i(\eta_i^T(t)Q\eta_i(t)) = (1 + \eta_i(t)^TQ\eta_i(t))^2, \end{cases} \quad (20)$$

where $\gamma_i > 0$ is a prescribed scalar.

Remark 3: From (20), it can be observed that each distributed platoon tracking control law $\tilde{u}_i(t)$ does not depend on any global information of the underlying digraph $\tilde{\mathcal{G}}$. Besides, all gain and weighting matrices L , F , K , and S can be determined offline without any global graph knowledge and independent of the platoon scale. Indeed, each platoon member i , $i \in \mathcal{V}$, adopts only the local information $\eta_i(t)$ from its neighbors, specified by the nonzero adjacency elements a_{ij} in (10), to regulate its motion. Therefore, the proposed distributed platooning control design procedure above is fully scalable for large and/or size-varying platoons. Such a scalability feature is also beneficial for undertaking flexible cooperative maneuvers such as platoon splitting and platoon merging that will be elaborated in the ensuing section.

Remark 4: Note that the time-varying coupling gain $\alpha_i(t)$ in (20) satisfies that $\alpha_i(t) \geq 1$ for all $t \geq 0$. As a matter of fact, by letting $\check{\alpha}_i(t) = \alpha_i(t) - 1$, it is easily derived that $\dot{\check{\alpha}}_i(t) = -\gamma_i\check{\alpha}_i(t) + \eta_i^T(t)S\eta_i(t)$. Therefore, we have that $\check{\alpha}_i = e^{-\gamma_i t}\check{\alpha}_i(0) + \int_0^t e^{-\gamma_i(t-\tau)}\eta_i^T(\tau)S\eta_i(\tau)d\tau \geq 0$ in view that $\check{\alpha}_i(0) = \alpha_i(0) - 1 \geq 0$. In addition, the smooth function $\rho_i(s) = (1 + s)^2$ is monotonically increasing and $\rho_i(s) \geq 1$ for any $s > 0$. These two time-varying functions aim to bring the adequate adaptiveness and extra degrees of design freedom into the scalable adaptive platoon tracking control protocol such that the uncertainties (unknown τ_i , w_i , v_i , m_i) resided in the vehicle longitudinal dynamics can be restrained in an accommodative manner.

D. Stability Analysis

We next present the stability analysis criterion of the error dynamics (13) and (16).

Theorem 1: For the vehicular platoon (2) over a generic V2V communication topology $\tilde{\mathcal{G}}$ satisfying Assumption 1, under the scalable and resilient platoon tracking control laws (20), all variables of the estimation error dynamics (13) and the tracking error dynamics (16) are uniformly ultimately bounded. Furthermore, the spacing error ψ_i on each follower vehicle converges to some small neighborhood around zero.

Proof: See Appendix.

Remark 5: To prove the boundedness of the estimation and tracking errors in (13) and (16), the Lyapunov functions independent on the specific communication topology are employed in the proof of Theorem 1. Therefore, when the digraph $\tilde{\mathcal{G}}$ is time-varying, this Lyapunov function can be used as a common Lyapunov function. Such an observation is key to perform the following stability analysis under switching topologies. Specifically, we denote by the time-varying communication digraph at time t by $\tilde{\mathcal{G}}_{\vartheta(t)}$, where $\vartheta(t) : [0, \infty) \rightarrow \Xi_S = \{1, 2, \dots, S\}$ is a piecewise constant switching signal with Ξ_S representing a finite set of digraphs over S vertices. It is assumed that there exists an infinite sequence of contiguous, nonempty, nonoverlapping, uniformly bounded time intervals, $[t_0, t_1], [t_1, t_2], \dots, [t_s, t_{s+1}], \dots$, such that the communication digraph $\tilde{\mathcal{G}}_s$ over each interval is fixed and the union of the digraphs satisfies Assumption 1. Then, for the platoon (2) over switching directed V2V communication topologies $\tilde{\mathcal{G}}_{\vartheta(t)}$, under the distributed platoon tracking control laws (20), all variables of the error dynamics (13) and (16) remain uniformly ultimately bounded.

Remark 6: The resulting error dynamic (13) and (16) provide a unified model for the full longitudinal vehicle state estimation, anomaly signal estimation, and resilient platoon behavior analysis via accommodating various communication topologies and uncertainties. However, due to the presence of the uncertainties, it is pervasively required to attenuate their effects on the platoon behavior and further ensure that their propagation along the upstream direction of the platoon is not amplified. A widely-explored performance criterion against disturbance propagation is string stability, which prevents disturbance amplification in the upstream direction of the platoon. However, it is noteworthy that the string stability of the concerned platoon (1) depends on not only the desired observer-based adaptive platoon tracking control law (9), but also the V2V communication topology and spacing policy. Since the main focus of this study is to develop a scalable and resilient distributed platoon tracking control approach that accounts for generic communication topologies and spacing policies, it is generally difficult to analyze the uniform string stability of the platoon as in the literature [5], [32]. Similar to [11], [13], the effects of the uncertainties aforementioned are not attenuated uniformly along the string, but suppressed adaptively.

Remark 7: Even though a linearized longitudinal dynamical model is employed in (1), the proposed adaptive platoon tracking control design method in Section III-B also can be exploited to deal with heterogeneous nonlinear longitudinal dynamics. For example, in the presence of various resistance forces, the longitudinal dynamics of the i -th vehicle can be described by the following force balance equation:

$$m_i \ddot{v}_i(t) = F_i^{en}(t) - F_i^{re}(t), \quad (21)$$

where m_i denotes the mass of vehicle i ; $F_i^{en}(t)$ represents the desired engine force acting on vehicle i ; and $F_i^{re}(t) = f_i^g(t) + f_i^a(t) + f_i^r(t)$ represents the lumped resistance forces.

Specifically, $f_i^g(t) = m_i g \sin(\alpha_i(t))$ denotes the gravity component parallel to the road surface with $\alpha_i(t)$ denoting the angle of inclination of the road; $f_i^a(t) = \frac{1}{2} \rho C_d A_f (\dot{p}_i(t) + v_w(t))^2$ denotes the air resistance force with ρ being the air density, A_f being the frontal area of the vehicle, C_d being the aerodynamic drag coefficient, and $v_w(t)$ being the headwind speed; and $f_i^r(t) = \mu m_i g \cos(\alpha_i(t))$ stands for the rolling resistance force with μ being the rolling resistance coefficient. Furthermore, by modeling the engine inertial delay as a first-order filter, the engine force can be given by $\tau_i \dot{F}_i^{en}(t) + F_i^{en}(t) = u_i^{en}(t)$, where $u_i^{en}(t) = m_i \ddot{u}_i(t)$ is the actual engine throttle/brake input of the i -th vehicle. Denoting $\chi_i(t) = -\frac{\tau_i}{m_i} (\dot{f}_i^g(t) + f_i^a(t) + f_i^r(t)) - \frac{1}{m_i} (f_i^g(t) + f_i^a(t) + f_i^r(t))$ and $w_i(t) = -\tilde{\tau}_i \ddot{p}_i(t)$, one further has that

$$\tau_e \ddot{p}_i(t) + \ddot{p}_i(t) = \tilde{u}_i(t) + \chi_i(t) + w_i(t), i \in \tilde{\mathcal{V}}. \quad (22)$$

Recalling (1) and (3), the nonlinear term $\chi_i(t)$ above with regard to the resistance forces then can be treated as an unknown input as $m_i(t)$ in (3). The rest analysis and design remain unchanged. In this sense, the effects of the uncertain nonlinear resistance forces on the platoon control system can be accurately estimated and properly compensated.

E. Scalable and Adaptive Platoon Maneuvers

Platooned vehicles, although operating within dedicated lanes, would demand various dynamic platoon maneuvers such as splitting and merging due to the changeable traffic conditions (e.g., obstacle/emergency vehicles) and individual destinations (e.g., highway entry and exit). Generally, precise platoon splitting and merging maneuvers require both longitudinal and lateral control efforts as well as management protocols for transient phases. However, the tight coupling and cooperation of the vehicle longitudinal and lateral control actions during a dynamic platoon maneuver render the theoretical investigation complicated. Although the decoupled dynamic models make a dynamic platoon maneuver possible via separately regulating longitudinal and lateral motions [33], there is an essential switching among different controllers, which may induce a loss of stability in the longitudinal closed-loop dynamics [19], [34]. In what follows, we show how the proposed scalable adaptive longitudinal control approach can be potentially adopted to account for the dynamic splitting and merging maneuvers of automated vehicular platoons.

1) *Platoon Splitting*: A typical strategy to deal with vehicle-leaving operations during vehicle platooning follows three steps: *i*) listening the splitting request(s); *ii*) reconfiguring the V2V communication links of the relevant platoon members to disengage the leaving vehicle(s); and *iii*) closing the inter-vehicle gaps left by the leaving vehicle(s). Furthermore, it is generally required to make safe steering and further lane changing to guarantee successful splitting. However, how actions including steering and lane changing are performed safely is beyond the scope of this study.

We next outline the main body of a *Split_Maneuver* algorithm for accomplishing platoon splitting tasks in the context of longitudinal control.

2) *Platoon Merging*: Similar to a splitting maneuver, a common strategy for handling vehicle-joining events may include the following four steps: *i*) listening the merging request(s); *ii*) opening the inter-vehicle gaps for the joining vehicle(s); *iii*)

Algorithm 1: The Main Part of *Split_Maneuver* Algorithm.

```

1: while  $t < T_{sim}$  do  $\triangleright T_{sim}$ : the simulation time
2:   Listen Split_Request, and record the leaving
      vehicle id  $S_i$  and the leaving time  $t_{S_i}$ 
3:   for  $i \in \mathcal{V}$  do
4:     if Split_Request = Nil OR  $t < t_{S_i}$  then
5:       Collect  $\{\hat{x}_j(t)\}$  over  $\tilde{\mathcal{G}} \rightarrow \eta_i(t)$  in (10)
6:       Derive  $\tilde{u}_i(t)$  in (20) and apply (3) to (2)
7:     else if  $t \geq t_{S_i}$  then  $\triangleright$  After splitting
8:       if  $i \neq S_i$  then
9:         Update  $\{d_j(t)\}$  for any  $j > S_i$ 
10:        Reconfigure the V2V links without  $S_i$ 
11:        Collect  $\{\hat{x}_j(t)\}$  over  $\tilde{\mathcal{G}} \rightarrow \eta_i(t)$  in (10)
12:        Derive  $\tilde{u}_i(t)$  in (20) and apply (3) to (2)
13:     end if
14:   end if
15: end for
16: end while

```

establishing and reconfiguring the V2V communication links due to the joining vehicle(s); and *iv*) letting the joining vehicle(s) merge in the convoy.

A stretch of a *Merge_Maneuver* algorithm is provided below.

Algorithm 2: The Main Part of *Merge_Maneuver* Algorithm.

```

1: while  $t < T_{sim}$  do  $\triangleright T_{sim}$ : the simulation time
2:   Listen Merge_Request, and record the vehicle id
       $M_i$  in front of which the merging vehicle  $J_i$  requests
      to join and the time  $t_{M_i}$  (in join-at-tail case:
       $J_i = N + 1$ )
3:   for  $i \in \mathcal{V}$  do
4:     if Merge_Request = Nil OR  $t < t_{M_i}$  then
5:       Collect  $\{\hat{x}_j(t)\}$  over  $\tilde{\mathcal{G}} \rightarrow \eta_i(t)$  in (10)
6:       Derive  $\tilde{u}_i(t)$  in (20) and apply (3) to (2)
7:     else if  $t \geq t_{M_i}$  then  $\triangleright$  After merging
8:       Update  $\{d_j(t)\}$  for any  $j \geq M_i$ 
9:       Add  $J_i$  to  $\tilde{\mathcal{G}}$  and reconfigure the V2V links with
       $J_i$ 
10:      Collect  $\{\hat{x}_j(t)\}$  over  $\tilde{\mathcal{G}} \rightarrow \eta_i(t)$  in (10)
11:      Derive  $\tilde{u}_i(t)$  in (20) and apply (3) to (2)
12:    end if
13:  end for
14:  if  $t \geq t_{M_i}$  then  $\triangleright$  For the merging vehicle  $J_i$ 
15:    Set  $d_{J_i}(t) \leftarrow d_{M_i}(t)$ 
16:    Configure the V2V links from/to  $J_i$  over  $\tilde{\mathcal{G}}$ 
17:    Collect  $\{\hat{x}_{J_i}(t)\}$  over  $\tilde{\mathcal{G}} \rightarrow \eta_{J_i}(t)$  in (10)
18:    Derive  $\tilde{u}_{J_i}(t)$  in (20) and apply (3) to (2)
19:  end if
20: end while

```

We note the following two points for the above algorithms:
1) depending on the V2V communication topology $\tilde{\mathcal{G}}$, the communication links affecting the relevant platoon members due to the leaving/joining vehicle(s) should be reconfigured on a case-by-case basis. For example, under the LF topology, no links

between the remaining platoon members need to be reconnected because the leaving vehicle S_i only receives information from the platoon leader. Under the PF topology, only the communication link between the predecessor and successor of the leaving vehicle S_i is required to be reconstructed. Whereas, it is out of scope of this paper to explore how these links are connected and reconfigured. It is thus assumed that the link reconfigurations are successfully completed at the splitting/merging time; and 2) the strategy of updating the formation vector $d_j(t)$ after the leaving/joining events rests on the spacing policy adopted for the platoon. For example, if a constant spacing is considered, then one has $d_j(t) = (j+1)d_0$ for $t \geq t_{S_i}$ and $j > S_i$ after vehicle leaving.

Before ending this section, we further remark that the splitting and merging events can be sporadic, concurrent and humongous during practical platoon maneuvering. We only consider the longitudinal platooning on an envisaged highway with an aim to verify the feasibility of automated platoon maneuvering under the scalable and resilient longitudinal platooning control approach. It is therefore not our ambition herein to classify the vast platoon maneuvers and explore exhaustively the maneuvering strategies.

IV. SIMULATION RESULTS

In this section, we conduct comprehensive case studies of different platoon maneuvers involving various uncertainties, such as heterogeneous engine time lags, time-varying disturbance, measurement noise, actuator anomaly, and leader control variation. The ultimate goal is to ensure that the platoon members can track and attain the specified velocity and acceleration of the platoon leader during the maneuvers, meanwhile guaranteeing the desired spacing requirement in the presence of the uncertainties.

The automated platoon, if not elsewhere specified, consists of one leader vehicle and ten follower vehicles. The desired spacing between any consecutive platoon members during normal platoon driving is set as 10 m. Each platoon maneuver in the subsequent cases starts with $p_0 = 100$ m, an initial cruise speed 5 m/s, and zero initial tracking errors. Furthermore, $D = 0.1$, $\kappa_1 = 0.5$ and $\kappa_2 = 2.1$. The initial value of $\alpha_i(t)$ is taken as $\alpha_i(0) = 1.3$ and $\gamma_i = 0.1$ for all $i \in \mathcal{V}$. The inertial time lags in the heterogeneous longitudinal dynamics (1) are assumed to be $\{\tau_i\}_{i=1}^{10} = \{0.6, 0.6, 0.7, 0.7, 0.75, 0.7, 0.6, 0.8, 0.8, 0.7\}$ s with $\tau_e = 0.6$ s.

A. A Resilient Platoon Driving Scenario

First, we consider a platoon driving scenario via evaluating the stability and resilience performance of the coordinated platoon under various uncertainties. Specifically, it is assumed that a sinusoidal external disturbance $w_i(t) = A_w \sin(\frac{2\pi}{10}(t - 20))$ with $A_w = 1.5$ m/s² is imposed on every platoon member $i \in \mathcal{V}$ during the period $t \in [20, 25]$ s. For each follower vehicle i , its position measurement is corrupted by a persistent noise $v_i(t)$ with its value randomly varied within $[-0.01, 0.01]$ m. The leader vehicle is commanded to accelerate gradually for about 33 s, then decelerate to a new speed 16.25 m/s and maintain this speed for the convoy afterwards. Such a leader command scheduling might be common during the overtaking and lane changing maneuvers, where the new lane permits a higher speed. We further suppose that some platoon members suffer from mechanical or electronic faults on throttle/brake

actuators. Specifically, it is assumed that the follower vehicle 2 experiences an abrupt and persistent bias fault $m_2(t) = -1.3$ m/s² from $t \geq 80$ s and the follower vehicle 5 experiences an abrupt and persistent bias fault $m_5(t) = 1.5$ m/s² from $t \geq 60$ s, and $m_i(t) = 0$ for the other vehicles $i \in \mathcal{V}/\{2, 5\}$.

With the local observer (8), each platoon member is capable to identify and estimate the unknown actuator anomaly $m_i(t)$. Then, the unfavorable effect of the misbehaved actuator on the internal stability of each vehicle and further the entire platoon stability can be compensated and adaptively resisted by the proposed platooning control strategy. The preliminary simulation tests show that the stability and safety of the maneuvered platoon in the above driving scenario can not be guaranteed over any V2V communication topologies in Fig. 1 if the anomaly estimation and compensation are not considered. However, following the design procedure in Section III-B, it is found that the proposed platooning control approach is effective to guarantee the stable and resilient platoon driving behavior over all V2V communication topologies in Fig. 1 by suitably choosing the design parameters. For brevity, we provide the simulation results over the PF topology only. By implementing the designed platoon tracking control law $\hat{u}_i(t)$ (under $V = 18$ I), Fig. 2 depicts the stable and resilient behaviors of the platoon driving maneuver in terms of the relative positions to the leader $\phi_i(t) = p_0(t) - p_i(t)$, velocities $\dot{p}_i(t)$, accelerations $\ddot{p}_i(t)$, position tracking errors $e_i^p(t) = p_i(t) - d_i(t) - p_0(t)$, and spacing errors $\psi_i(t) = p_{i-1}(t) - p_i(t) - d_{i-1,i}(t)$. It can be seen that 1) the imposed external disturbance $w_i(t)$ on every platoon member causes their accelerations to fluctuate over time during $t \in [20, 25]$, as depicted in Fig. 2(c). Their shockwave effects, however, are then effectively attenuated by the proposed adaptive platooning control laws within an acceptable period of time; 2) the variations of the leader control command $u_0(t)$ also lead to certain transient performance degradation, as can be observed in Fig. 2(c) at times 30 s, 40 s, 50 s, and 60 s, respectively. Nevertheless, due to the adaptivity nature of the proposed platooning control laws, such degraded performance can be recovered soon; and 3) the injected actuator faults $m_2(t)$ and $m_5(t)$ induce relatively steep changes into the accelerations near their occurrence times. However, owing to the promising fault estimation and compensation features of the designed observers, the adverse faulty effects can be rapidly suppressed and accommodated, as can be clearly seen in Fig. 2(a)–(e). Furthermore, Fig. 2(f)–(i) show the adaptive control inputs $u_i(t)$ and coupling gains $\alpha_i(t)$, and the fault estimates $\hat{m}_2(t)$ and $\hat{m}_5(t)$, respectively. Obviously, the computed control variables and the adaptive coupling gains are confined within some bounds. Also, the simulated actuator faults are well estimated by the designed observers.

The simulation results above substantiate that the proposed scalable adaptive platooning control approach can not only maneuver a fleet of cooperative vehicles to perform the desired platoon driving task but also serve as an effective means for guaranteeing the resilience requirement during practical platoon maneuvers in harsh environments against the simultaneous unknown disturbances, measurement noises, actuator anomaly, and leader control input changes.

B. A Resilient Platoon Splitting Scenario

Next, we examine a platoon splitting maneuver with dynamic leaving vehicles under the same uncertain environments of the

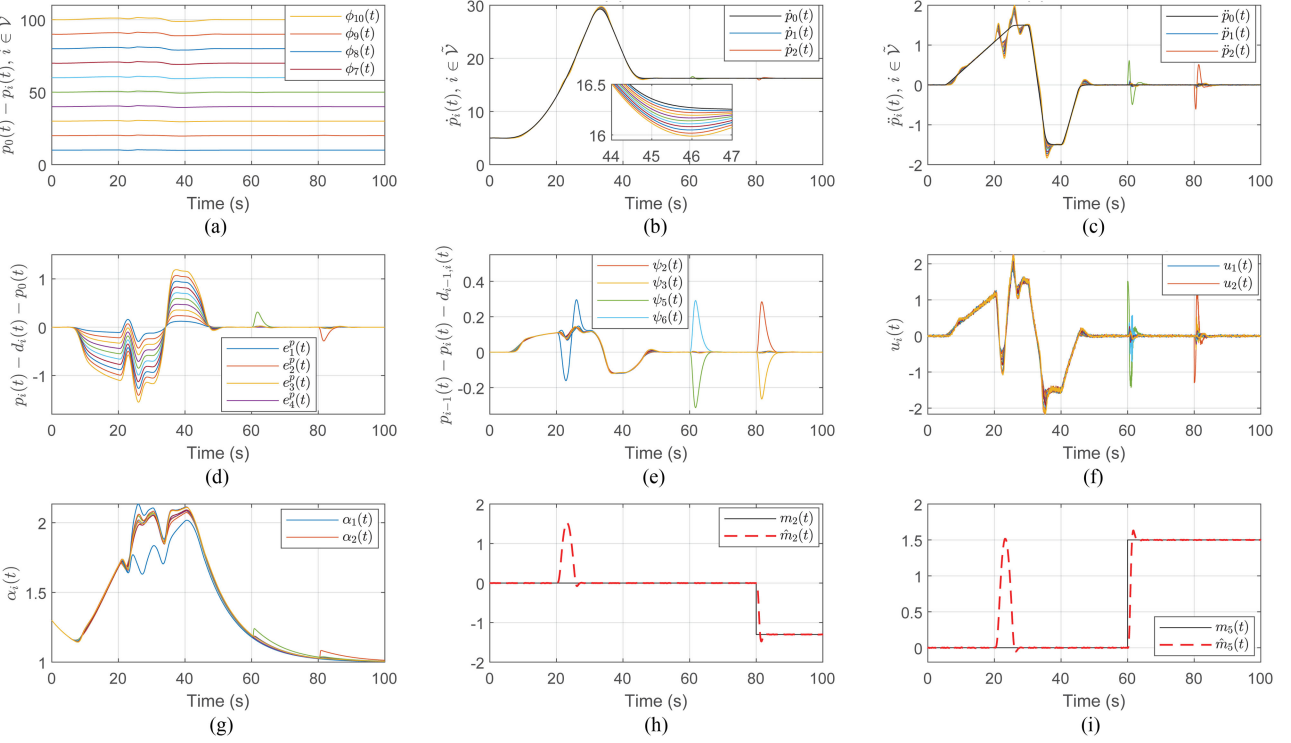


Fig. 2. Stability and resilience of the platoon driving maneuver over the PF V2V communication topology in the presence of sinusoidal external disturbances $w_i(t) = 1.5 \sin(\frac{2\pi}{10}(t - 20))$, $t \in [20, 25]$ s, persistent random measurement noises $v_i(t) \in [-0.01, 0.01]$ for all $i \in \mathcal{V}$, and actuator faults $m_2(t) = -1.3$, $t \geq 80$ s and $m_5(t) = 1.5$, $t \geq 60$ s.

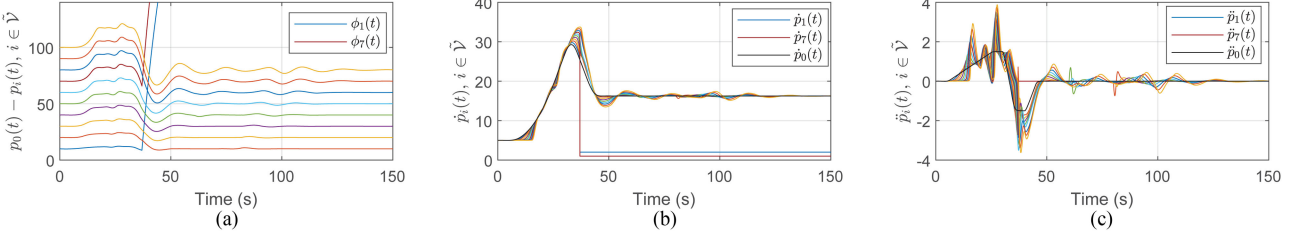


Fig. 3. Trajectories of vehicle relative positions to the leader, velocities, and accelerations during the platoon splitting maneuver over the PF communication topology in the presence of external disturbances $w_i(t)$, measurement noises $v_i(t)$, and actuator faults $m_2(t)$ and $m_5(t)$, $i \in \mathcal{V}$, where the follower vehicles Veh_1 and Veh_7 simultaneously leave the platoon at $t = 37$ s.

driving scenario examined above. We test the proposed platooning control approach over the PF topology, while the tests over the other V2V communication topologies can be similarly performed. The commonly explored splitting scenarios include: single leave-at-tail maneuver, single leave-at-middle maneuver, and multiple leaving maneuver. Since the tail vehicle does not broadcast its information to the other vehicles of the platoon over the PF topology, the single leave-at-tail maneuver is then straightforward by removing the leaving vehicle from the convoy at the splitting time.

In what follows, it is assumed that the first platoon member Veh_1 and the seventh platoon member Veh_7 intend to leave the platoon simultaneously at time $t = 37$ s, and such a leaving operation is decisive and safe for the two vehicles to change the lane. Note that each platoon member over the PF topology only receives information from its predecessor, which implies that the leaving vehicles Veh_1 and Veh_7 are required to inform

their predecessors and successors for disconnecting the relevant communication links, and their predecessors and successors should also get well notified by the leaving vehicles of their leaving intent and be prepared for “reconnecting” without the splitting vehicles. Since the proposed platooning control strategy is mainly responsible for the longitudinal maneuver, the focus of the subsequent simulation is to evaluate whether the proposed platooning control strategy is capable of effectively and adaptively regulating the longitudinal space gaps left by the leaving vehicles Veh_1 and Veh_7 from $t = 37$ s, while at the same time maintaining the stability and resilience requirements for the platoon afterwards. By applying the designed observer-based platoon tracking control law $\tilde{u}_i(t)$ (under $V = 0.05I$), Fig. 3 shows the relative positions to the leader $\phi_i(t)$, velocities $\dot{\phi}_i(t)$, and accelerations $\ddot{\phi}_i(t)$ of the platoon, where we can see that 1) the spacing gaps left by Veh_1 and Veh_7 are adequately and promptly closed under the adaptive control laws; and 2)

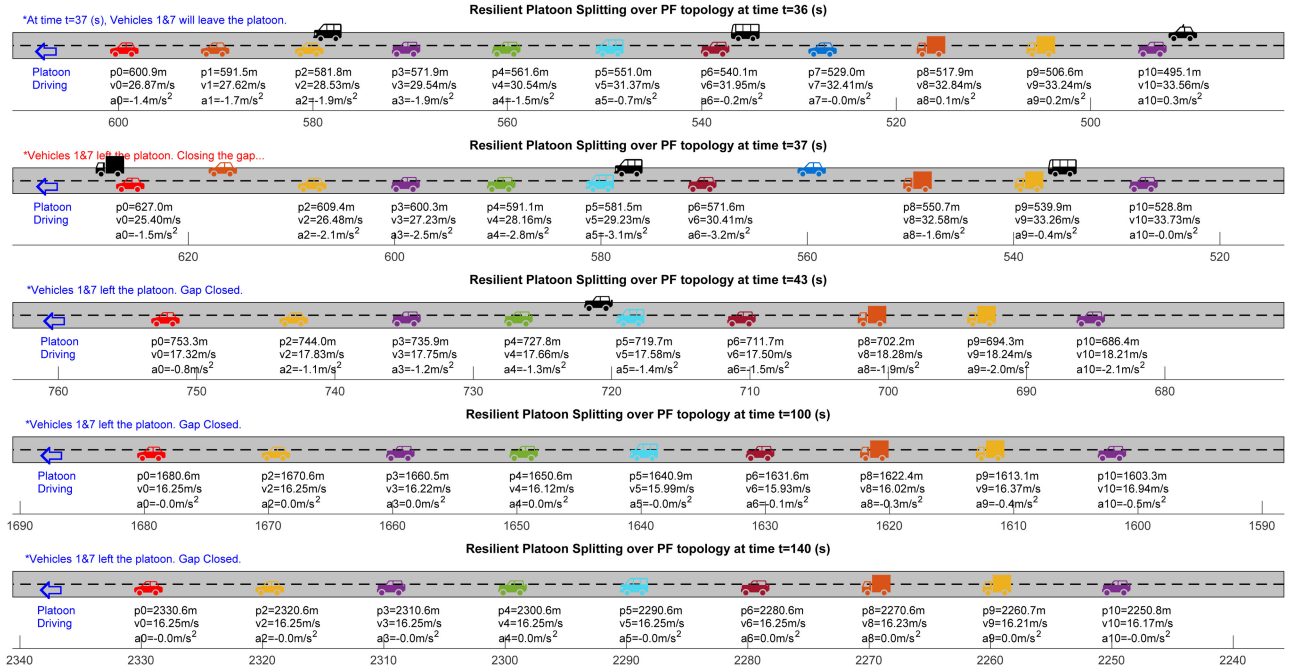


Fig. 4. Snapshots of the simulated platoon splitting maneuver, where the follower vehicles Veh_1 and Veh_7 simultaneously leave the platoon and perform a lane change at $t = 37$ s, and then travel at constant speeds 2 m/s and 1 m/s, respectively (platoon vehicles: color; non-platoon vehicles: black; real-time position p_i , velocity $\dot{p}_i = v_i$ and acceleration $\ddot{p}_i = a_i$, $i \in \bar{\mathcal{V}} = \{0, 1, \dots, 10\}$).

the remaining platoon is capable to preserve both the desired stability and resilience.

To further provide an intuitionistic evaluation, we develop a simulative two-lane platoon maneuvering environment, which simulates and visualizes the motions of the vehicles on a straight and flat two-lane road. The snapshots of the simulated platoon splitting maneuver over the PF V2V communication topology before and after splitting are provided in Fig. 4, where the platoon members Veh_1 and Veh_7 change the platoon lane (bottom lane) to a non-platoon lane (top lane) at $t = 37$ s, and then travel at constant and lower speeds 2 m/s and 1 m/s, respectively. At approximately $t = 43$ s the spacing gaps caused by the leaving vehicles are effectively reduced to approximately 10 m, and the platoon well maintains the desired spacing, stability, and resilience requirements during the remaining simulation time, which confirms the effectiveness of the proposed adaptive platooning control laws.

C. A Resilient Platoon Merging Scenario

Finally, we proceed to evaluate a resilient platoon merging scenario with dynamic joining vehicles under the same uncertain environments aforementioned. Similar to the splitting events, some common merging scenarios include: single join-at-tail maneuver, single join-at-middle maneuver, and multiple joining maneuver. In what follows, we consider a platoon merging maneuver with two joining vehicles (of the same type of the platoon leader vehicle) over the PF topology. Specifically, the first joining vehicle Veh_{11} requests to merge at the tail of the platoon at time $t = 90$ s and the second joining vehicle Veh_{12} requests to merge in front of the platoon member Veh_6 at time $t = 35$ s.

Before letting the joining vehicles merge in the platoon, the associated platoon members usually need to open a suitable

inter-vehicle gap, thereby creating certain safety distance for the joining vehicles. For this purpose, we assume that the joining vehicle Veh_{12} will wait for two seconds within its initial lane for the platoon members Veh_5 and Veh_6 creating the safety distance. Therefore, the actual merging time of vehicle Veh_{12} in the platoon is at $t = 37$ s. We next test the efficiency and effectiveness of the proposed adaptive platooning control strategy over the PF topology on adjusting the longitudinal space gaps for the joining vehicles from their merging times and preserving the stability and resilience for the expanded platoon afterwards. Implementing the designed control law $\tilde{u}_i(t)$ (under $V = 0.06I$), the simulation results are presented in Figs. 5 and 6, where Fig. 5 depicts the relative positions to the leader, velocities $\dot{p}_i(t)$, and accelerations $\ddot{p}_i(t)$ of the platooned vehicles, and Fig. 6 demonstrates the temporal snapshots of the simulated platoon merging maneuver.

It can be observed from Fig. 6 that the spacing gap between platoon members Veh_5 and Veh_6 at $t = 35$ s is 11.2 m, while the gap increases to 13.8 m at $t = 37$ s. This means that if the joining vehicle Veh_{12} merges in the middle of the gap at $t = 35$ s, the inter-vehicle distance between the related vehicles is about 5.6 m, which may not be safe enough in some practical situation. Whereas, the inter-vehicle gap is efficiently opened to 6.9 m within two seconds, and thus offers more safety requirement for performing the merging operation. The snapshot at time 48 s also indicates that the proposed adaptive platooning control strategy can quickly settle down the newly merged vehicle as a platoon member. On the other hand, the results in Figs. 5 and 6 suggest that the designed adaptive controllers are remarkably resilient to the concerned uncertainties and provide guaranteed stability and robustness for the expanded platoon during the harsh merging maneuver.

The demonstration video of the simulated driving, splitting, and merging scenarios above within the developed simulative

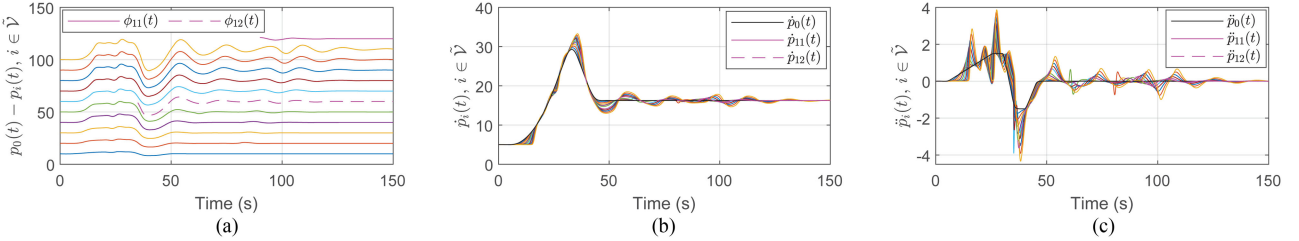


Fig. 5. Trajectories of vehicle relative positions to the leader, velocities, and accelerations during the platoon merging maneuver over the PF communication topology in the presence of external disturbances $w_i(t)$, measurement noises $v_i(t)$, and actuator faults $m_2(t)$ and $m_5(t)$, $i \in \mathcal{V}$, where two vehicles Veh_{11} and Veh_{12} merge the platoon at $t = 90$ s and $t = 37$ s, respectively.

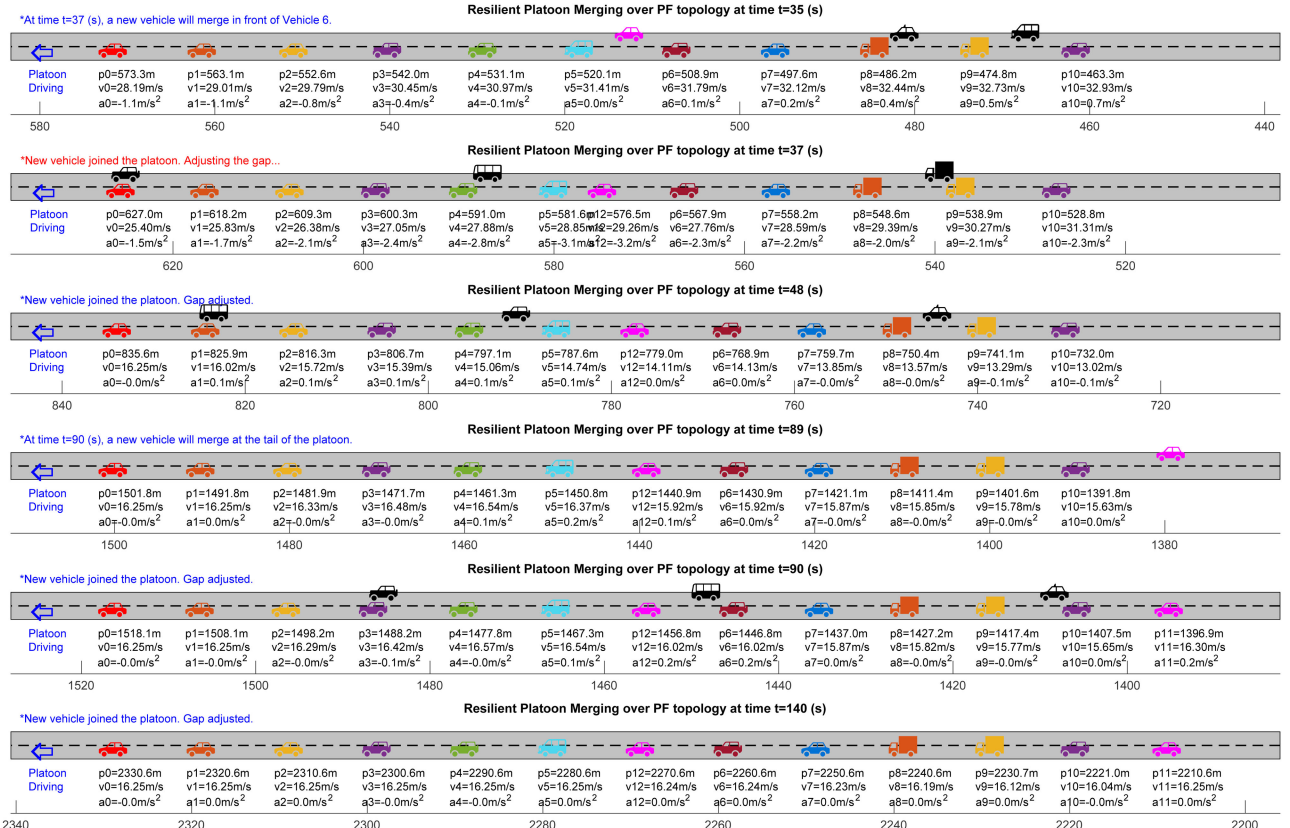


Fig. 6. Snapshots of the simulated platoon merging maneuver, where the vehicle Veh_{11} joins at the tail of the platoon at $t = 90$ s and the vehicle Veh_{12} joins in front of the platoon member 6 at $t = 37$ s (platoon vehicles: color; merging vehicles: magenta; non-platoon vehicles: black; real-time position p_i , velocity $p_i = v_i$ and acceleration $p_i = a_i$, $i \in \mathcal{V} = \{0, 1, \dots, 12\}$).

two-lane platoon maneuvering environment can be found at <https://www.youtube.com/watch?v=HUQpj4rqUqQ>.

V. CONCLUSION

The scalable and resilient longitudinal control problem of a platoon of CACC-based connected and automated vehicles is addressed. First, a general longitudinal vehicle model is established, in the presence of unknown heterogeneous engine inertial delays, external disturbances, measurement noises, and actuator anomaly on follower vehicles, and also the unknown control input on the platoon leader. A scalable adaptive platooning control approach is proposed with guaranteed platoon stability and resilience against the uncertainties over generic

V2V communication topologies and spacing policies. A formal stability analysis of the estimation errors, platoon tracking errors and spacing errors is provided. It is demonstrated through comprehensive simulations that the proposed scalable and resilient platooning control approach is promising to implement several elementary platoon maneuvers including platoon driving, splitting, and merging, while maintaining satisfactory platoon stability and resilience requirements.

APPENDIX PROOF OF THEOREM 1

We first consider the Lyapunov function candidate $V_{1,i} = \xi_i^T \tilde{P} \xi_i$. In view of (13), the time derivative of V_1 is calculated as

$\dot{V}_{1,i} = 2\xi_i^T \tilde{P} \dot{\xi}_i = 2\xi_i^T \tilde{P} \tilde{A} \xi_i + 2\xi_i^T \tilde{P} \tilde{E} \tilde{w}_i$. By Young's inequality, its last term is bounded as $2\xi_i^T \tilde{P} \tilde{E} \tilde{w}_i \leq \frac{1}{\beta_0} \xi_i^T \tilde{P} \tilde{E} \tilde{E}^T \tilde{P} \xi_i + \beta_0 \tilde{w}_i^T \tilde{w}_i$, where β_0 is some positive scalar. To ensure the boundedness of all controlled variables in the resulting estimation error dynamics (13), without loss of generality, the disturbance input w_i , the measurement noise v_i in (7), and the derivative of the anomaly signal $\dot{m}_i(t)$ are supposed to be continuous and bounded; i.e., $\|w_i(t)\| \leq \bar{w}$, $\|v_i(t)\| \leq \bar{v}$, and $\|\dot{m}_i(t)\| \leq \bar{m}$, where \bar{w}, \bar{v} , and \bar{m} denote some positive constants that are not necessarily known. Then, we have that $\dot{V}_{1,i} \leq \xi_i^T (\tilde{P} \tilde{A} + \tilde{A}^T \tilde{P} + \frac{1}{\beta_0} \tilde{P} \tilde{E} \tilde{E}^T \tilde{P}) \xi_i + \beta_0 \tilde{w}_i^T \tilde{w}_i \leq -\xi_i^T U \xi_i + \bar{\epsilon}_2 \leq -\epsilon_1 V_{1,i} + \bar{\epsilon}_2$, where $\epsilon_1 = \frac{\lambda(U)}{\lambda(\tilde{P})}$, $\bar{\epsilon}_2 = \beta_0(\bar{w}^2 + \bar{v}^2 + \bar{m}^2)$, and (17) is used. Then, it is easy to get that $V_{1,i}(t) \leq e^{-\epsilon_1(t-t_0)} V_{1,i}(t_0) + \frac{\bar{\epsilon}_2}{\epsilon_1}$, which further implies that $\lim_{t \rightarrow \infty} V_{1,i}(t) \leq \frac{\bar{\epsilon}_2}{\epsilon_1}$. From the construction of $V_{1,i}(t)$, it is thus clear that ξ_i is bounded. Subsequently, one can deduce the uniform ultimate boundedness of $x_i, m_i, \hat{x}_i, \hat{m}_i$ for all $i \in \mathcal{V}$. Furthermore, $\xi_i^T \tilde{P} \xi_i \geq \underline{\lambda}(\tilde{P}) \|\xi_i\|^2$ implies that $\lim_{t \rightarrow \infty} \|\xi_i(t)\| \leq \bar{\xi} = \sqrt{\frac{\bar{\epsilon}_2}{\epsilon_1 \underline{\lambda}(\tilde{P})}}$. Thus, the bounds of the estimation errors \tilde{x}_i and \tilde{m}_i can be made small via suitably adjusting the values of ϵ_1 and $\bar{\epsilon}_2$ as well as the matrix \tilde{P} .

We next choose the following Lyapunov function candidate $V_2 = \sum_{i=1}^N \frac{\alpha_i}{6q_i} ((1 + \eta_i^T Q \eta_i)^3 - 1) + \sum_{i=1}^N \frac{1}{q_i} \tilde{\alpha}_i^2$, where $\tilde{\alpha}_i = \alpha_i - \bar{\alpha}_i$ with $\bar{\alpha}_i$ being a constant to be specified later. Calculating the time derivative of V_2 yields $\dot{V}_2 = \sum_{i=1}^N \frac{\dot{\alpha}_i}{q_i} (1 + \eta_i^T Q \eta_i)^2 \eta_i^T Q \dot{\eta}_i + \sum_{i=1}^N \frac{\dot{\alpha}_i}{6q_i} ((1 + \eta_i^T Q \eta_i)^3 - 1) + 2 \sum_{i=1}^N \frac{1}{q_i} \tilde{\alpha}_i \dot{\tilde{\alpha}}_i$. Considering the tracking error dynamics (16), the first term of \dot{V}_2 is estimated as $\sum_{i=1}^N \frac{\dot{\alpha}_i}{q_i} (1 + \eta_i^T Q \eta_i)^2 \eta_i^T Q \dot{\eta}_i = \eta^T (\alpha \rho \mathcal{T} \otimes Q) \dot{\eta} = \eta^T (\alpha \rho \mathcal{T} \otimes Q A) \eta - \eta^T (\alpha \rho \mathcal{T} \mathcal{H} \alpha \rho \otimes Q B B^T Q) \eta + \eta^T (\alpha \rho \mathcal{T} \mathcal{H} \otimes Q L C) \tilde{x} + \eta^T (\alpha \rho \mathcal{T} \mathcal{H} \otimes Q) \varpi \leq \eta^T (\alpha \rho \mathcal{T} \otimes Q A) \eta - \frac{\lambda_0}{2} \eta^T (\alpha^2 \rho^2 \otimes S) \eta + \eta^T (\alpha \rho \mathcal{T} \mathcal{H} \otimes Q L C) \tilde{x} + \eta^T (\alpha \rho \mathcal{T} \mathcal{H} \otimes Q) \varpi$, where $\lambda_0 = \underline{\lambda}(G)$ and Lemma 1 is used the last " \leq ".

On the other hand, it holds that $\sum_{i=1}^N \frac{\dot{\alpha}_i}{q_i} ((1 + \eta_i^T Q \eta_i)^3 - 1) = \sum_{i=1}^N \frac{\eta_i^T S \eta_i}{6q_i} ((1 + \eta_i^T Q \eta_i)^3 - 1) - \sum_{i=1}^N \frac{\gamma_i(\alpha_i - 1)}{6q_i} ((1 + \eta_i^T Q \eta_i)^3 - 1) \leq \sum_{i=1}^N \frac{\eta_i^T S \eta_i}{6q_i} ((\eta_i^T Q \eta_i)^3 + 3(\eta_i^T Q \eta_i)^2 + 3\eta_i^T Q \eta_i) \leq \sum_{i=1}^N \frac{1}{2q_i \lambda_0^{\frac{3}{4}}} \eta_i^T Q \eta_i (1 + \eta_i^T Q \eta_i)^2 \eta_i^T S \eta_i \leq \sum_{i=1}^N \left(\frac{1}{8q_i^4 \lambda_0^3} + \frac{3}{8} \lambda_0 (\eta_i^T Q \eta_i)^{\frac{2}{3}} (1 + \eta_i^T Q \eta_i)^{\frac{1}{3}} \right) \eta_i^T S \eta_i \leq \sum_{i=1}^N \left(\frac{1}{8q_i^4 \lambda_0^3} + \frac{3}{8} \lambda_0 (\eta_i^T Q \eta_i)^4 \right) \eta_i^T S \eta_i \leq \sum_{i=1}^N \left(\frac{1}{8q_i^4 \lambda_0^3} + \frac{3}{8} \lambda_0 \rho_i^2 \right) \eta_i^T S \eta_i \leq \sum_{i=1}^N \frac{1}{8q_i^4 \lambda_0^3} \eta_i^T S \eta_i + \frac{3}{8} \lambda_0 \alpha_i^2 \rho_i^2 \eta_i^T S \eta_i \leq \sum_{i=1}^N \frac{1}{8q_i^4 \lambda_0^3} \eta_i^T S \eta_i + \frac{3}{8} \lambda_0 \eta^T (\alpha^2 \rho^2 \otimes S) \eta$. Then, we have $\dot{V}_2 \leq \eta^T (\alpha \rho \mathcal{T} \otimes Q A) \eta - \frac{\lambda_0}{2} \eta^T (\alpha^2 \rho^2 \otimes S) \eta + \eta^T (\alpha \rho \mathcal{T} \mathcal{H} \otimes Q L C) \tilde{x} + \eta^T (\alpha \rho \mathcal{T} \mathcal{H} \otimes Q) \varpi + \sum_{i=1}^N \frac{\eta_i^T S \eta_i}{8q_i^4 \lambda_0^3} + \frac{3}{8} \lambda_0 \eta^T (\alpha^2 \rho^2 \otimes S) \eta + 2 \sum_{i=1}^N \frac{1}{q_i} \tilde{\alpha}_i \dot{\tilde{\alpha}}_i = \eta^T (\alpha \rho \mathcal{T} \otimes Q A) \eta + \sum_{i=1}^N \left(-\frac{\lambda_0}{16} \alpha_i^2 \rho_i^2 + \frac{1}{8q_i^4 \lambda_0^3} + \frac{2\bar{\alpha}_i}{q_i} \right) \eta_i^T S \eta_i - 2 \sum_{i=1}^N \frac{1}{q_i} \gamma_i \tilde{\alpha}_i (\alpha_i - 1) - \frac{1}{16} \lambda_0 \eta^T (\alpha^2 \rho^2 \otimes S) \eta + \eta^T (\alpha \rho \mathcal{T} \mathcal{H} \otimes Q L C) \tilde{x} + \eta^T (\alpha \rho \mathcal{T} \mathcal{H} \otimes Q) \varpi = \eta^T (\alpha \rho \mathcal{T} \otimes Q A) \eta + \sum_{i=1}^N \left(-\frac{\lambda_0}{16} \alpha_i^2 \rho_i^2 - \frac{36}{\lambda_0 q_i^2} + \frac{2\alpha_i}{q_i} - \left(\frac{2\bar{\alpha}_i}{q_i} - \frac{1}{8q_i^4 \lambda_0^3} - \frac{36}{\lambda_0 q_i^2} \right) \right) \eta_i^T S \eta_i - 2 \sum_{i=1}^N \frac{1}{q_i} (\tilde{\alpha}_i^2 + \tilde{\alpha}_i (\bar{\alpha}_i - 1)) - \frac{1}{16} \lambda_0 \eta^T (\alpha^2 \rho^2 \otimes S) \eta + \eta^T (\alpha \rho \mathcal{T} \mathcal{H} \otimes Q L C) \tilde{x} + \eta^T (\alpha \rho \mathcal{T} \mathcal{H} \otimes Q) \varpi$

$Q) v \leq \eta^T (\alpha \rho \mathcal{T} \otimes Q A) \eta + \sum_{i=1}^N \left(-3 \frac{\alpha_i \rho_i}{q_i} + 2 \frac{\alpha_i \rho_i}{q_i} \right) \eta_i^T S \eta_i + \sum_{i=1}^N \frac{\gamma_i}{q_i} (-\tilde{\alpha}_i^2 + (\bar{\alpha}_i - 1)^2) - \frac{1}{16} \lambda_0 \eta^T (\alpha^2 \rho^2 \otimes S) \eta + \eta^T (\alpha \rho \mathcal{T} \mathcal{H} \otimes Q L C) \tilde{x} + \eta^T (\alpha \rho \mathcal{T} \mathcal{H} \otimes Q) \varpi \leq \eta^T (\alpha \rho \mathcal{T} \otimes (Q A - S)) \eta + \sum_{i=1}^N \frac{\gamma_i}{q_i} (-\tilde{\alpha}_i^2 + (\bar{\alpha}_i - 1)^2) - \frac{1}{16} \lambda_0 \eta^T (\alpha^2 \rho^2 \otimes S) \eta + \eta^T (\alpha \rho \mathcal{T} \mathcal{H} \otimes Q L C) \tilde{x} + \eta^T (\alpha \rho \mathcal{T} \mathcal{H} \otimes Q) \varpi$, where the inequalities $\frac{\lambda_0}{16} \alpha_i^2 \rho_i^2 + \frac{36}{\lambda_0 q_i^2} \geq \frac{3\alpha_i \rho_i}{q_i}$ and $\bar{\alpha}_i \geq \frac{1}{16q_i^3 \lambda_0^3} - \frac{18}{\lambda_0 q_i}$ are used to get the second " \leq " above. By Young's inequality, the last two terms can be bounded as $\eta^T (\alpha \rho \mathcal{T} \mathcal{H} \otimes Q L C) \tilde{x} \leq \frac{\beta_1}{2} \eta^T (\alpha^2 \rho^2 \mathcal{T} \mathcal{H} \mathcal{H}^T \mathcal{T}^T \otimes I_n) \eta + \frac{1}{2\beta_1} \tilde{x}^T (I_N \otimes C^T L^T Q^2 L C) \tilde{x}$ and $\eta^T (\alpha \rho \mathcal{T} \mathcal{H} \otimes Q) \varpi \leq \frac{\beta_2}{2} \eta^T (\alpha^2 \rho^2 \mathcal{T} \mathcal{H} \mathcal{H}^T \mathcal{T}^T \otimes I_n) \eta + \frac{1}{2\beta_2} \varpi^T (I_N \otimes Q^2) \varpi$, where $\beta_m > 0$, $m = 5, 6$, are prescribed constants. Furthermore, it is easy to derive that $\frac{1}{2\beta_1} \tilde{x}^T (I_N \otimes C^T L^T Q^2 L C) \tilde{x} \leq \frac{1}{2\beta_1} (\bar{\sigma}(Q L C))^2 \|\tilde{x}\|^2 \leq \frac{1}{2\beta_1} (\bar{\sigma}(Q L C))^2 \bar{\xi}^2$. Then, denoting $\varrho_2 = \sum_{i=1}^N \frac{\gamma_i}{q_i} (\bar{\alpha}_i - 1)^2 + \frac{1}{2\beta_1} (\bar{\sigma}(Q L C))^2 \bar{\xi}^2 + \frac{1}{2\beta_2} \varpi^T (I_N \otimes Q^2) \varpi$, we obtain that $\dot{V}_2 \leq \eta^T (\alpha \rho \mathcal{T} \otimes (Q A - S)) \eta - \frac{1}{16} \lambda_0 \eta^T (\alpha^2 \rho^2 \otimes S) \eta + \varrho_2 + \frac{1}{2} (\beta_1 + \beta_2) \eta^T (\alpha^2 \rho^2 \mathcal{T} \mathcal{H} \mathcal{H}^T \mathcal{T}^T \otimes I_n) \eta - \sum_{i=1}^N \frac{\gamma_i}{q_i} \tilde{\alpha}_i^2 \leq -\frac{1}{2} \eta^T (\alpha \rho \mathcal{T} \otimes V) \eta - \sum_{i=1}^N \frac{\gamma_i}{q_i} \tilde{\alpha}_i^2 + \varrho_2 - \left(\frac{1}{16} \lambda_0 \alpha^2 \rho^2 \underline{\sigma}(S) - \frac{1}{2} (\beta_1 + \beta_2) \bar{\alpha}^2 \bar{\rho}^2 \bar{\sigma}(\mathcal{T} \mathcal{H})^2 \right) \|\eta\|^2 \leq -\frac{1}{2} \eta^T (\alpha \rho \mathcal{T} \otimes V) \eta - \sum_{i=1}^N \frac{\gamma_i}{q_i} \tilde{\alpha}_i^2 + \varrho_2 \leq -\sum_{i=1}^N \frac{\alpha_i \rho_i}{2q_i} \underline{\lambda}(V) \eta_i^T \eta_i - \sum_{i=1}^N \frac{\gamma_i}{q_i} \tilde{\alpha}_i^2 + \varrho_2 \leq -\sum_{i=1}^N \frac{\alpha_i \lambda}{2q_i} \underline{\lambda}(Q^{-1}) \underline{\lambda}(V) \rho_i \eta_i^T Q \eta_i - \sum_{i=1}^N \frac{\gamma_i}{q_i} \tilde{\alpha}_i^2 + \varrho_2 \leq -\sum_{i=1}^N \frac{\alpha_i \lambda}{6q_i} \underline{\lambda}(Q^{-1}) \underline{\lambda}(V) ((1 + \eta_i^T Q \eta_i)^3 - 1) - \sum_{i=1}^N \frac{\gamma_i}{q_i} \tilde{\alpha}_i^2 + \varrho_2 \leq -\varrho_1 V_2 + \varrho_2$, where $\beta_1 + \beta_2 \leq \frac{8}{\bar{\sigma}(\mathcal{T} \mathcal{H})^2 \bar{\alpha}^2 \bar{\rho}^2}$ is used for the third " \leq ", and $\varrho_1 = \min\{\underline{\lambda}(Q^{-1}) \underline{\lambda}(V), \gamma_1, \gamma_2, \dots, \gamma_N\}$. Similarly, it is assumed that $\|\tilde{u}_0(t)\| \leq \bar{u}_0$, and $\|d(t)\| \leq \bar{d}$, where $\bar{m}, \bar{d} > 0$. Then we have $\varrho_2 \leq \bar{\varrho}_2 = \sum_{i=1}^N \frac{\gamma_i}{q_i} (\bar{\alpha}_i - 1)^2 + \frac{1}{2\beta_1} (\bar{\sigma}(Q L C))^2 \bar{\xi}^2 + \frac{\bar{\lambda}(Q^2) \bar{\lambda}(H)}{2\beta_2} (\bar{\sigma}(B) \bar{u}_0^2 + \bar{d}^2 + \bar{\sigma}(L D) \bar{v}^2)$ and $\lim_{t \rightarrow \infty} V_2(t) \leq \frac{\bar{\varrho}_2}{\varrho_1}$. Hence, all the controlled variables in the platoon tracking error dynamics, including $\alpha_i, \eta_i, \delta_i, x_i, x_0, e_i$, and u_i , are uniformly ultimately bounded.

Furthermore, by noting $V = \sum_{i=1}^N V_{1,i} + V_2$, we have that $V \geq \underline{\lambda}(\tilde{P}) \|\xi\|^2 + \sum_{i=1}^N \frac{\alpha_i}{6q_i} ((\eta_i^T Q \eta_i)^2 + 3(\eta_i^T Q \eta_i) + 3) \eta_i^T Q \eta_i \geq \underline{\lambda}(\tilde{P}) \|\xi\|^2 + \frac{1}{2\bar{q}} \sum_{i=1}^N \eta_i^T Q \eta_i \geq \frac{\varsigma}{2} (\|\xi\|^2 + \|\delta\|^2) \geq \frac{\varsigma}{2} (\|\tilde{x}\|^2 + \|\delta\|^2) \geq \frac{\varsigma}{2} \|\delta - \tilde{x}\|^2 = \frac{\varsigma}{2} \|e\|^2 = \frac{\varsigma}{2} \|x - \mathbf{1} \otimes x_0 - d\|^2$, where $\bar{q} = \max\{q_1, q_2, \dots, q_N\}$, $\varsigma = \min\{2\underline{\lambda}(\tilde{P}), \frac{\underline{\lambda}(\mathcal{H})^2 \underline{\lambda}(Q)}{\bar{q}}\}$. Then, one obtains $\lim_{t \rightarrow \infty} \|x(t) - \mathbf{1} \otimes x_0(t) - d(t)\| \leq \sqrt{\frac{2\bar{\epsilon}_2}{\varsigma \epsilon_1} + \frac{2\bar{\varrho}_2}{\varsigma \varrho_1}}$, which indicates that the bound of platoon tracking error $e_i = x_i - x_0 - d_i$ and further the spacing error ψ_i can be regulated to some neighborhoods around zero via suitably adjusting the values of $\varsigma, \epsilon_1, \bar{\epsilon}_2, \varrho_1$, and $\bar{\varrho}_2$. This completes the proof.

REFERENCES

- [1] P. Jootel, "Safe road trains for the environment," SARTRE Project, Final Project Report, Oct. 2012. [Online]. Available: <http://www.sartre-project.eu/en/publications/Sidor/default.aspx>
- [2] E. V. Nunen, M. R. J. A. E. Kwakernaak, J. Ploeg, and B. D. Netten, "Cooperative competition for future mobility," *IEEE Trans. Intell. Transp. Syst.*, vol. 13, no. 3, pp. 1018–1025, Sep. 2012.
- [3] Z. Wang, G. Wu, M. Barth, Y. Bian, S. Li, and S. Shladover, "A survey on cooperative longitudinal motion control of multiple connected and automated vehicles," *IEEE Intell. Transp. Syst. Mag.*, vol. 12, no. 1, pp. 4–24, Spring 2020.

- [4] R. Rajamani, *Vehicle Dynamics and Control*. 2nd ed. Berlin, Germany: Springer-Verlag, 2012.
- [5] J. Ploeg, D. P. Shukla, N. van de Wouw, and H. Nijmeijer, "Controller synthesis for string stability of vehicle platoons," *IEEE Trans. Intell. Transp. Syst.*, vol. 15, no. 2, pp. 854–865, Apr. 2014.
- [6] G. Guo, P. Li, and L.-Y. Hao, "Adaptive fault-tolerant control of platoons with guaranteed traffic flow stability," *IEEE Trans. Veh. Technol.*, vol. 69, no. 7, pp. 6916–6927, Jul. 2020.
- [7] F. Ma *et al.*, "Distributed control of cooperative vehicular platoon with nonideal communication condition," *IEEE Trans. Veh. Technol.*, vol. 69, no. 8, pp. 8207–8300, Aug. 2020.
- [8] I. Herman, S. Knorn, and A. Ahlén, "Disturbance scaling in bidirectional vehicle platoons with different asymmetry in position and velocity coupling," *Automatica*, vol. 82, pp. 13–20, Aug. 2017.
- [9] S. Wen and G. Guo, "Control of leader-following vehicle platoons with varied communication range," *IEEE Trans. Intell. Veh.*, vol. 5, no. 2, pp. 240–250, Jun. 2020.
- [10] M. Pirani, E. Hashemi, J. Simpson-Porco, B. Fidan, and A. Khajepour, "Graph theoretic approach to the robustness of k -nearest neighbor vehicle platoons," *IEEE Trans. Intell. Transp. Syst.*, vol. 18, no. 11, pp. 3218–3224, Nov. 2017.
- [11] Y. Zheng, S. Li, K. Li, and W. Ren, "Platooning of connected vehicles with undirected topologies: Robustness analysis and distributed h-infinity controller synthesis," *IEEE Trans. Intell. Transp. Syst.*, vol. 19, no. 5, pp. 1353–1364, May 2018.
- [12] J. Hu, P. Bhowmick, F. Arvin, A. Lanzon, and B. Lennox, "Cooperative control of heterogeneous connected vehicle platoons: An adaptive leader-following approach," *IEEE Robot. Autom. Lett.*, vol. 5, no. 2, pp. 977–984, Apr. 2020.
- [13] S. Wen and G. Guo, "Sampled-data control for connected vehicles with markovian switching topologies and communication delay," *IEEE Trans. Intell. Transp. Syst.*, vol. 21, no. 7, pp. 2930–2942, Jul. 2020.
- [14] S. Li, X. Qin, Y. Zheng, J. Wang, K. Li, and H. Zhang, "Distributed platoon control under topologies with complex eigenvalues: Stability analysis and controller synthesis," *IEEE Trans. Control Syst. Technol.*, vol. 27, no. 1, pp. 206–220, Jan. 2019.
- [15] Y. Li, C. Tang, S. Peeta, and Y. Wang, "Nonlinear consensus-based connected vehicle platoon control incorporating car-following interactions and heterogeneous time delays," *IEEE Trans. Intell. Transp. Syst.*, vol. 20, no. 6, pp. 2209–2219, Jun. 2019.
- [16] S. Xiao, X. Ge, Q.-L. Han, and Y. Zhang, "Secure distributed adaptive platooning control for automated vehicles over vehicular ad-hoc networks under DoS attacks," *IEEE Trans. Cybern.*, to be published, doi: [10.1109/TCYB.2021.3074318](https://doi.org/10.1109/TCYB.2021.3074318).
- [17] C. Zhao, X. Duan, L. Cai, and P. Cheng, "Vehicle platooning with non-ideal communication networks," *IEEE Trans. Veh. Technol.*, vol. 70, no. 1, pp. 18–32, Jan. 2021.
- [18] X. Ge, S. Xiao, Q.-L. Han, X.-M. Zhang, and D. Ding, "Dynamic event-triggered scheduling and platooning control co-design for automated vehicles over vehicular ad-hoc networks," *IEEE/CAA J. Autom. Sin.*, vol. 9, no. 1, pp. 31–46, Jan. 2022.
- [19] S. Santini, A. Salvi, A. Valente, A. Pescapè, M. Segata, and R. Lo Cigno, "Platooning maneuvers in vehicular networks: A distributed and consensus-based approach," *IEEE Trans. Intell. Veh.*, vol. 4, no. 1, pp. 59–72, Mar. 2019.
- [20] D. Bevly *et al.*, "Lane change and merge maneuvers for connected and automated vehicles: A survey," *IEEE Trans. Intell. Veh.*, vol. 1, no. 1, pp. 105–120, Mar. 2016.
- [21] R. Oliveira, C. Montez, A. Boukerche, and M. Wangham, "Co-design of consensus-based approach and reliable communication protocol for vehicular platoon control," *IEEE Trans. Veh. Technol.*, vol. 70, no. 9, pp. 9510–9524, Sep. 2021.
- [22] S. Parkinson, P. Ward, K. Wilson, and J. Miller, "Cyber threats facing autonomous and connected vehicles: Future challenges," *IEEE Trans. Intell. Transp. Syst.*, vol. 18, no. 11, pp. 2898–2915, Nov. 2017.
- [23] Researchers hack into driverless car system, take control of vehicle, Accessed: May 1, 2015. [Online]. Available: <https://www.nationaldefensemagazine.org/articles/2015/5/1/2015may-researchers-hack-into-driverless-car-system-take-control-of-vehicle>
- [24] Y. Liu, D. Yao, H. Li, and R. Lu, "Distributed cooperative compound tracking control for a platoon of vehicles with adaptive NN," *IEEE Trans. Cybern.*, to be published, doi: [10.1109/TCYB.2020.3044883](https://doi.org/10.1109/TCYB.2020.3044883).
- [25] Z. Yang, J. Huang, D. Yang, and Z. Zhong, "Collision-free ecological cooperative robust control for uncertain vehicular platoons with communication delay," *IEEE Trans. Veh. Technol.*, vol. 70, no. 3, pp. 2153–2166, Mar. 2021.
- [26] Y. Zhu, D. Zhao, and Z. Zhong, "Adaptive optimal control of heterogeneous CACC system with uncertain dynamics," *IEEE Trans. Control Syst. Technol.*, vol. 27, no. 4, pp. 1772–1779, Jul. 2019.
- [27] S. Feng, H. Sun, Y. Zhang, J. Zheng, H. Liu, and L. Li, "Tube-based discrete controller design for vehicle platoons subject to disturbances and saturation constraints," *IEEE Trans. Control Syst. Technol.*, vol. 28, no. 3, pp. 1066–1073, May 2020.
- [28] Y. Harfouch, S. Yuan, and S. Baldi, "An adaptive switched control approach to heterogeneous platooning with intervehicle communication losses," *IEEE Trans. Control Netw. Syst.*, vol. 5, no. 3, pp. 1434–1444, Sep. 2018.
- [29] A. Lopes and R. Araújo, "Active fault diagnosis method for vehicles in platoon formation," *IEEE Trans. Veh. Technol.*, vol. 69, no. 4, pp. 3590–3603, Apr. 2020.
- [30] H. Zhang and F. Lewis, "Adaptive cooperative tracking control of higher-order nonlinear systems with unknown dynamics," *Automatica*, vol. 48, no. 7, pp. 1432–1439, Jul. 2012.
- [31] K. Gu, V. Kharitonov, and J. Chen, *Stability of Time-delay Systems*, Boston, MA, USA: Springer Science & Business Media, 2003.
- [32] S. Stüdli, M. Seron, and R. Middleton, "From vehicular platoons to general networked systems: String stability and related concepts," *Annu. Rev. Control*, vol. 44, pp. 157–172, Oct. 2017.
- [33] P. Liu, A. Kurt, and U. Ozguner, "Distributed model predictive control for cooperative and flexible vehicle platooning," *IEEE Trans. Control Syst. Technol.*, vol. 27, no. 3, pp. 1115–1128, May 2019.
- [34] D. Liberzon, *Switching in Systems and Control*. Berlin, Germany: Springer Science & Business Media, 2012.



Xiaohua Ge (Senior Member, IEEE) received the B.Eng. degree in electronics and information engineering from Nanchang Hangkong University, Nanchang, China, in 2008, the M.Eng. degree in control theory and control engineering from Hangzhou Dianzi University, Hangzhou, China, in 2011, and the Ph.D. degree in computer engineering from Central Queensland University, Rockhampton, QLD, Australia, in 2014. From 2011 to 2013, he was a Research Assistant with the Centre for Intelligent and Networked Systems, Central Queensland University, where he was a Research Fellow in 2014. From 2015 to 2017, he was a Research Fellow with the Griffith School of Engineering, Griffith University, Gold Coast, QLD, Australia. He is currently a Senior Lecturer with the School of Science, Computing and Engineering Technologies, Swinburne University of Technology, Melbourne, VIC, Australia. His research interests include networked, secure, intelligent control and estimation theories, and their applications in electric vehicles, autonomous vehicles, and connected vehicles.

Dr. Ge was the recipient of The 2021 IEEE/CAA Journal of Automatica Sinica Norbert Wiener Review Award and 2019 IEEE Systems, Man, and Cybernetics Society Andrew P. Sage Best Transactions Paper Award. He is an Associate Editor for IEEE TRANSACTIONS ON SYSTEMS, MAN, AND CYBERNETICS: SYSTEMS. He is also an Early Career Advisory Board Member of IEEE/CAA JOURNAL OF AUTOMATICA SINICA and was a Guest Editor of several Special Issues.



Qing-Long Han (Fellow, IEEE) received the B.Sc. degree in mathematics from Shandong Normal University, Jinan, China, in 1983, and the M.Sc. and Ph.D. degrees in control engineering from the East China University of Science and Technology, Shanghai, China, in 1992 and 1997, respectively. He is currently the Pro Vice-Chancellor (Research Quality) and a Distinguished Professor with the Swinburne University of Technology, Melbourne, VIC, Australia. He held various academic and management positions with Griffith University, QLD, Australia, and Central Queensland University, Rockhampton, QLD, Australia. His research interests include networked control systems, multi-agent systems, time-delay systems, smart grids, unmanned surface vehicles, and neural networks.

Prof. Han was the recipient of the 2021 Norbert Wiener Award (the Highest Award in systems science and engineering, and cybernetics), 2021 M. A. Sargent Medal (the Highest Award of the Electrical College Board of Engineers Australia), 2021 IEEE/CAA Journal of Automatica Sinica Norbert Wiener Review Award, 2020 IEEE Systems, Man, and Cybernetics (SMC) Society Andrew P. Sage Best Transactions Paper Award, 2020 IEEE Transactions on Industrial Informatics Outstanding Paper Award, and 2019 IEEE SMC Society Andrew P. Sage Best Transactions Paper Award.

Prof. Han is a Member of the Academia Europaea (The Academy of Europe) and Fellow of The Institution of Engineers Australia. He is a Highly Cited Researcher in both Engineering and Computer Science (Clarivate Analytics, 2019–2021). He was an AdCom Member of IEEE Industrial Electronics Society (IES), IES Fellow Committee, and the Chair of IEEE IES Technical Committee on Networked Control Systems. He is the Co-Editor-in-Chief of IEEE TRANSACTIONS ON INDUSTRIAL INFORMATICS, Deputy Editor-in-Chief of the IEEE/CAA JOURNAL OF AUTOMATICA SINICA, Co-Editor of *Australian Journal of Electrical and Electronic Engineering*, an Associate Editor for 12 international journals, including IEEE TRANSACTIONS ON CYBERNETICS, IEEE Industrial Electronics Magazine, Control Engineering Practice, and Information Sciences, and a Guest Editor of 13 Special Issues.



Xian-Ming Zhang (Senior Member, IEEE) received the M.Sc. degree in applied mathematics and the Ph.D. degree in control theory and control engineering from Central South University, Changsha, China, in 1992 and 2006, respectively. From 2007 to 2014, he was a Postdoctoral Research Fellow and a Lecturer with the School of Engineering and Technology, Central Queensland University, Rockhampton, QLD, Australia. From 2014 to 2016, he was a Lecturer with the Griffith School of Engineering, Griffith University, Gold Coast, QLD, Australia. In 2016, he joined the Swinburne University of Technology, Melbourne, VIC, Australia, where he is currently an Associate Professor with the School of Science, Computing, and Engineering Technologies. His research interests include H-infinity filtering, event-triggered control systems, networked control systems, neural networks, multi-agent systems, offshore platforms and time-delay systems.

He was the recipient of second National Natural Science Award in China in 2013, jointly with Prof. M. Wu and Prof. Y. He. He was also the recipient of The 2021 IEEE/CAA Journal of Automatica Sinica Norbert Wiener Review Award, 2020 IEEE TRANSACTIONS ON INDUSTRIAL INFORMATICS Outstanding Paper Award, 2019 IEEE Systems, Man, and Cybernetics Society Andrew P. Sage Best Transactions Paper Award, and 2016 IET Control Theory and Applications Premium Award. He is an Associate Editor for IEEE TRANSACTIONS ON CYBERNETICS, *Journal of the Franklin Institute, International Journal of Control, Automation, and Systems, Neurocomputing, and Neural Processing Letters*.



Jun Wang (Life Fellow, IEEE) received the B.S. degree in electrical engineering and the M.S. degree in systems engineering from the Dalian University of Technology, Dalian, China, and the Ph.D. degree in systems engineering from Case Western Reserve University Cleveland, OH, USA. He held various academic positions with the Dalian University of Technology, Case Western Reserve University, University of North Dakota, Grand Forks, ND, USA, and the Chinese University of Hong Kong, Hong Kong. He also held various short-term or part-time

visiting positions with USAF Armstrong Laboratory, Dayton, OH, USA, RIKEN Brain Science Institute, Tokyo, Japan, Huazhong University of Science and Technology, Wuhan, China, Shanghai Jiao Tong University, Shanghai, China, and Dalian University of Technology. He is currently a Chair Professor with the Department of Computer Science and School of Data Science, City University of Hong Kong, Hong Kong. He was the Editor-in-Chief of IEEE TRANSACTIONS ON CYBERNETICS during 2014–2019 and an Associate Editor for the journal and its predecessor during 2003–2013. He was also with the Editorial Board or Editorial Advisory Board of IEEE TRANSACTIONS ON NEURAL NETWORKS, IEEE TRANSACTIONS ON SYSTEMS, MAN, AND CYBERNETICS, PART C, *Neural Networks*, and a *International Journal of Neural Systems*. He was a Guest Editor of special issues of *European Journal of Operational Research*, *International Journal of Neural Systems*, and *Neurocomputing*. He was the General Chair of the IEEE World Congress on Computational Intelligence in 2008, 13th and 25th International Conference on Neural Information Processing in 2006 and 2018.

Prof. Wang is a Fellow of the International Association for Pattern Recognition and a Foreign Member of Academia Europaea. He was the recipient of the Research Excellence Award from The Chinese University of Hong Kong, Hong Kong, for 2008–2009, Outstanding Achievement Award from Asia Pacific Neural Network Assembly, IEEE TRANSACTIONS ON NEURAL NETWORKS Outstanding Paper Award in 2011, Neural Networks Pioneer Award from the IEEE Computational Intelligence Society in 2014, Norbert Wiener Award from the IEEE Systems, Man and Cybernetics Society in 2019, among other distinctions.